Today's outline - November 13, 2024

Today's outline - November 13, 2024

- HAXPES Experiments

Today's outline - November 13, 2024

- HAXPES Experiments
- X-ray magnetic circular dichroism

Today's outline - November 13, 2024

- HAXPES Experiments
- X-ray magnetic circular dichroism
- Resonant Scattering

Today's outline - November 13, 2024

- HAXPES Experiments
- X-ray magnetic circular dichroism
- Resonant Scattering
- Bijvoet (Bay-voot) Pairs

Today's outline - November 13, 2024

- HAXPES Experiments
- X-ray magnetic circular dichroism
- Resonant Scattering
- Bijvoet (Bay-voot) Pairs
- MAD Phasing

Today's outline - November 13, 2024

- HAXPES Experiments
- X-ray magnetic circular dichroism
- Resonant Scattering
- Bijvoet (Bay-voot) Pairs
- MAD Phasing
- Quantum Origin of Resonant Scattering

Today's outline - November 13, 2024

- HAXPES Experiments
- X-ray magnetic circular dichroism
- Resonant Scattering
- Bijvoet (Bay-voot) Pairs
- MAD Phasing
- Quantum Origin of Resonant Scattering

Reading Assignment: Chapter 8.5-8.7

Today's outline - November 13, 2024

- HAXPES Experiments
- X-ray magnetic circular dichroism
- Resonant Scattering
- Bijvoet (Bay-voot) Pairs
- MAD Phasing
- Quantum Origin of Resonant Scattering

Reading Assignment: Chapter 8.5-8.7

Homework Assignment #06:
Chapter 6: 1,6,7,8,9
due Friday, November 15, 2024

Today's outline - November 13, 2024

- HAXPES Experiments
- X-ray magnetic circular dichroism
- Resonant Scattering
- Bijvoet (Bay-voot) Pairs
- MAD Phasing
- Quantum Origin of Resonant Scattering

Reading Assignment: Chapter 8.5-8.7

Homework Assignment #06:
Chapter 6: 1,6,7,8,9
due Friday, November 15, 2024

Please send me your choices for General User proposal and final exam presentation. I need to approve them by the end of the week!

The photoemission process

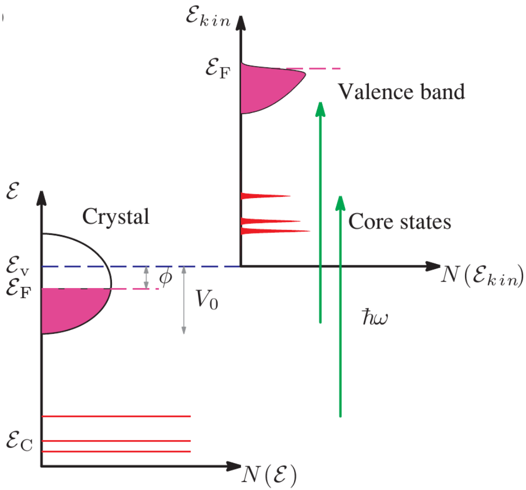

With the incident photon energy, $\hbar\omega$, held constant, an analyzer is used to measure the kinetic energy, $\mathcal{E}_{kin}$, of the photoelectrons emitted from the surface of the sample

The photoemission process

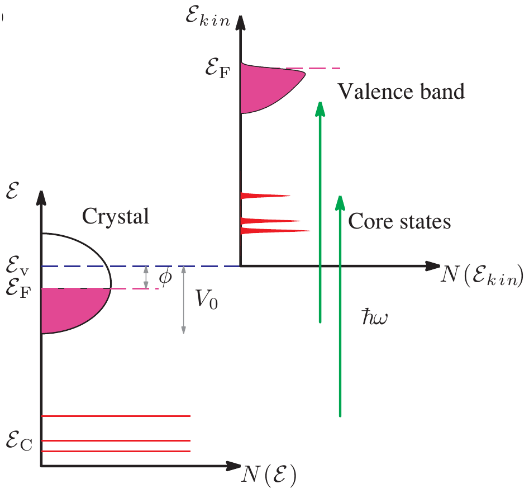

With the incident photon energy, $\hbar\omega$, held constant, an analyzer is used to measure the kinetic energy, $\mathcal{E}_{kin}$, of the photoelectrons emitted from the surface of the sample

if $\mathcal{E}_i$ is the initial energy of the electron, the binding energy, $\mathcal{E}_B$ is

The photoemission process

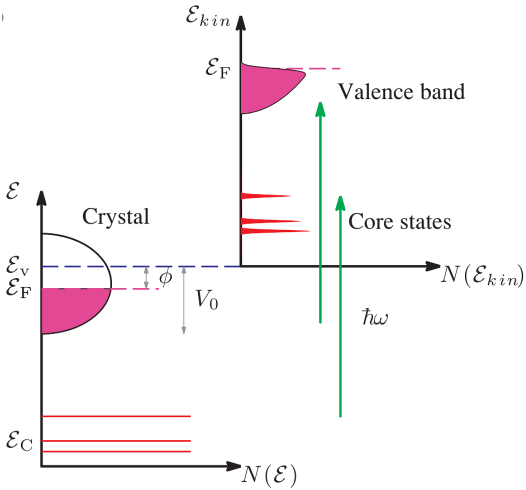

With the incident photon energy, $\hbar\omega$, held constant, an analyzer is used to measure the kinetic energy, $\mathcal{E}_{kin}$, of the photoelectrons emitted from the surface of the sample

if $\mathcal{E}_i$ is the initial energy of the electron, the binding energy, $\mathcal{E}_B$ is

$$\mathcal{E}_B = \mathcal{E}_F - \mathcal{E}_i$$

The photoemission process

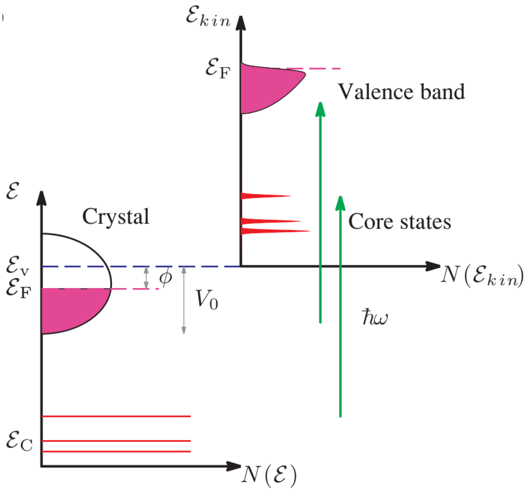

With the incident photon energy, $\hbar\omega$, held constant, an analyzer is used to measure the kinetic energy, $\mathcal{E}_{kin}$, of the photoelectrons emitted from the surface of the sample

if $\mathcal{E}_i$ is the initial energy of the electron, the binding energy, $\mathcal{E}_B$ is

$$\mathcal{E}_B = \mathcal{E}_F - \mathcal{E}_i$$

and the measured kinetic energy gives the binding energy

The photoemission process

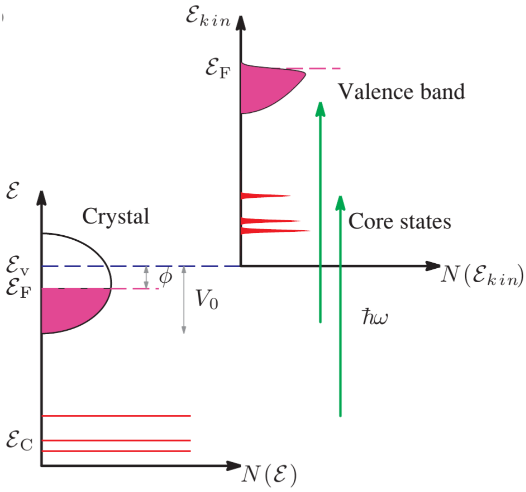

With the incident photon energy, $\hbar\omega$, held constant, an analyzer is used to measure the kinetic energy, $\mathcal{E}_{kin}$, of the photoelectrons emitted from the surface of the sample

if $\mathcal{E}_i$ is the initial energy of the electron, the binding energy, $\mathcal{E}_B$ is

$$\mathcal{E}_B = \mathcal{E}_F - \mathcal{E}_i$$

and the measured kinetic energy gives the binding energy

$$\mathcal{E}_{kin} = \frac{\hbar^2 q_v^2}{2m}$$

The photoemission process

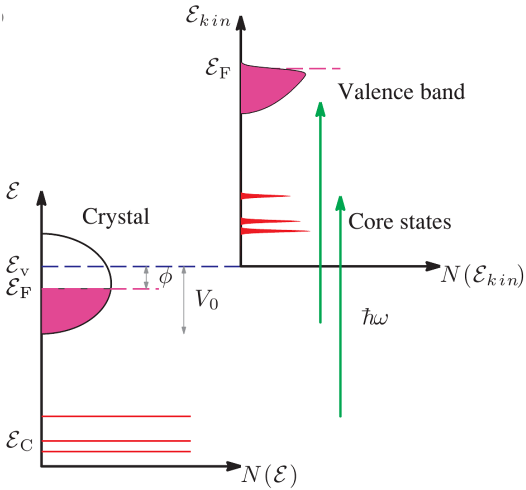

With the incident photon energy, $\hbar\omega$, held constant, an analyzer is used to measure the kinetic energy, $\mathcal{E}_{kin}$, of the photoelectrons emitted from the surface of the sample

if $\mathcal{E}_i$ is the initial energy of the electron, the binding energy, $\mathcal{E}_B$ is

$$\mathcal{E}_B = \mathcal{E}_F - \mathcal{E}_i$$

and the measured kinetic energy gives the binding energy

$$\mathcal{E}_{kin} = \frac{\hbar^2 q_v^2}{2m} = \hbar\omega - \phi - \mathcal{E}_B$$

The photoemission process

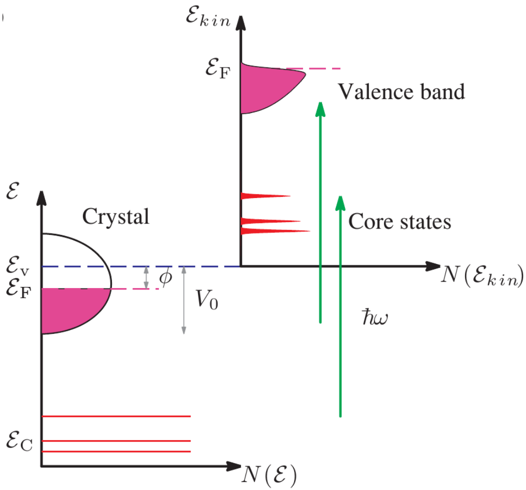

With the incident photon energy, $\hbar\omega$, held constant, an analyzer is used to measure the kinetic energy, $\mathcal{E}_{kin}$, of the photoelectrons emitted from the surface of the sample

if $\mathcal{E}_i$ is the initial energy of the electron, the binding energy, $\mathcal{E}_B$ is

$$\mathcal{E}_B = \mathcal{E}_F - \mathcal{E}_i$$

and the measured kinetic energy gives the binding energy

$$\mathcal{E}_{kin} = \frac{\hbar^2 q_v^2}{2m} = \hbar\omega - \phi - \mathcal{E}_B$$

the maximum kinetic energy measured is thus related to the Fermi energy

The photoemission process

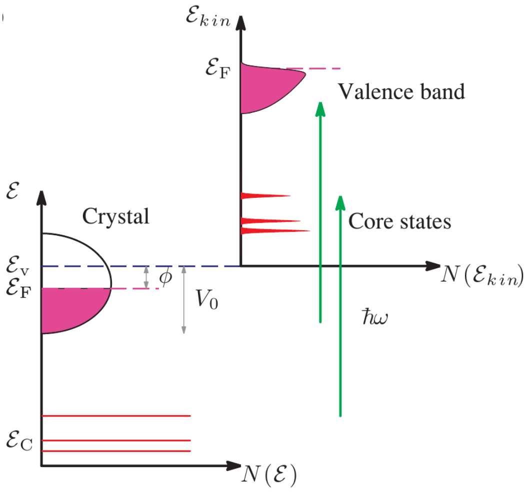

With the incident photon energy, $\hbar\omega$, held constant, an analyzer is used to measure the kinetic energy, $\mathcal{E}_{kin}$, of the photoelectrons emitted from the surface of the sample

if $\mathcal{E}_i$ is the initial energy of the electron, the binding energy, $\mathcal{E}_B$ is

$$\mathcal{E}_B = \mathcal{E}_F - \mathcal{E}_i$$

and the measured kinetic energy gives the binding energy

$$\mathcal{E}_{kin} = \frac{\hbar^2 q_v^2}{2m} = \hbar\omega - \phi - \mathcal{E}_B$$

the maximum kinetic energy measured is thus related to the Fermi energy

the core states are used to fingerprint the chemical composition of the sample

Hemispherical mirror analyzer

The electric field between the two hemispheres of radius R_1 and R_2 has a R^2 dependence from the center of the hemispheres

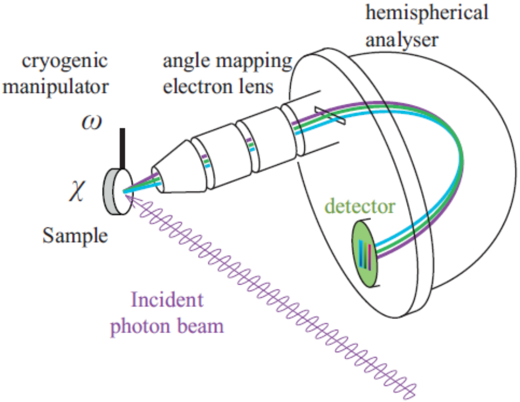

Hemispherical mirror analyzer

The electric field between the two hemispheres of radius R_1 and R_2 has a R^2 dependence from the center of the hemispheres

Electrons with $\mathcal{E}_0$, called the "pass energy", will follow a circular path of radius

$$R_0 = (R_1 + R_2)/2$$

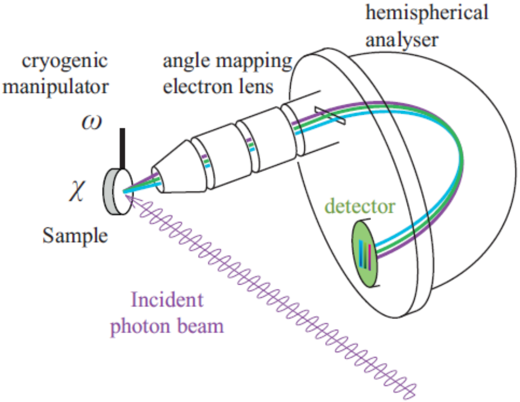

Hemispherical mirror analyzer

The electric field between the two hemispheres of radius R_1 and R_2 has a R^2 dependence from the center of the hemispheres

Electrons with $\mathcal{E}_0$, called the "pass energy", will follow a circular path of radius

$$R_0 = (R_1 + R_2)/2$$

Electrons with lower energy will fall inside this circular path while those with higher energy will fall outside

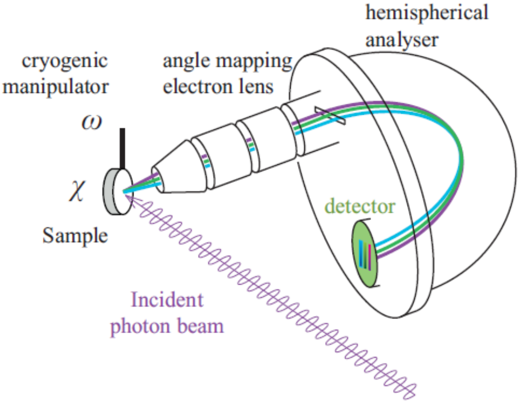

Hemispherical mirror analyzer

The electric field between the two hemispheres of radius R_1 and R_2 has a R^2 dependence from the center of the hemispheres

Electrons with $\mathcal{E}_0$, called the "pass energy", will follow a circular path of radius

$$R_0 = (R_1 + R_2)/2$$

Electrons with lower energy will fall inside this circular path while those with higher energy will fall outside

Electrons with different azimuthal exit angles ω will map to different positions on the 2D detector

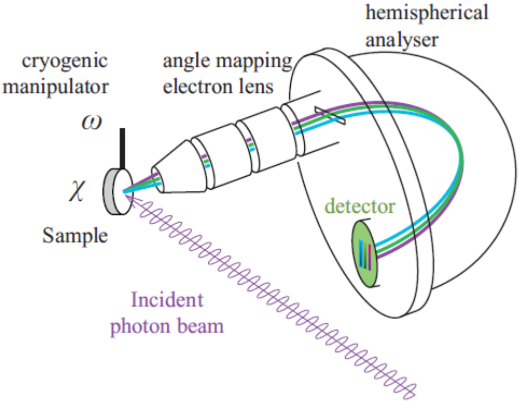

Photoelectron momentum

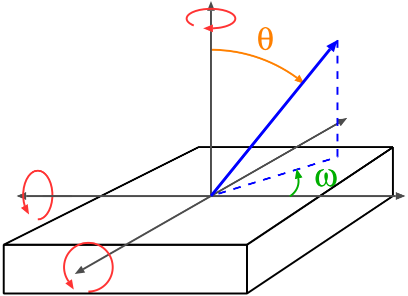

Photoelectron momentum

The total momentum of the photoelectron is calculated from the measured kinetic energy

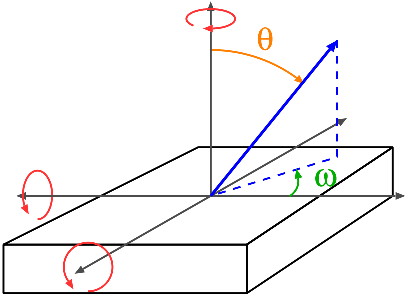

Photoelectron momentum

The total momentum of the photoelectron is calculated from the measured kinetic energy

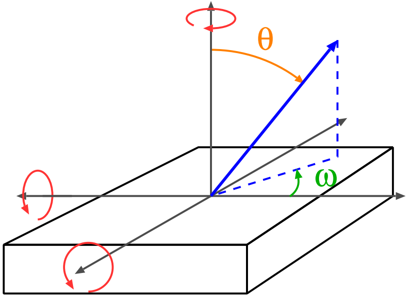

$$\hbar q_e = \sqrt{2m\mathcal{E}_{kin}}$$

Photoelectron momentum

The total momentum of the photoelectron is calculated from the measured kinetic energy

since the momentum of the electron parallel to the surface must be conserved, the original momentum of the electron can be computed from the polar angle of the sample to the detector and the azimuthal angle measured on the 2D detector

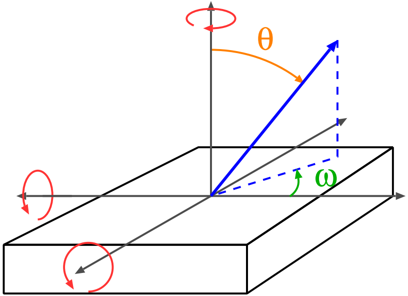

$$\hbar q_e = \sqrt{2m\mathcal{E}_{kin}}$$

Photoelectron momentum

The total momentum of the photoelectron is calculated from the measured kinetic energy

since the momentum of the electron parallel to the surface must be conserved, the original momentum of the electron can be computed from the polar angle of the sample to the detector and the azimuthal angle measured on the 2D detector

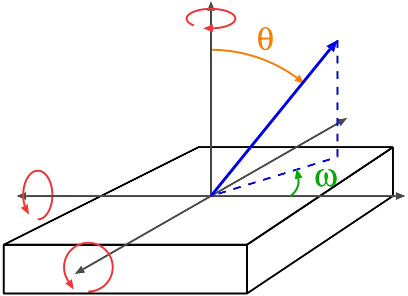

$$\hbar q_e = \sqrt{2m\mathcal{E}_{kin}}$$

$$\hbar q_{\|x} = \hbar q_e \sin\theta \cos\omega$$

$$\hbar q_{\|y} = \hbar q_e \sin\theta \sin\omega$$

Photoelectron momentum

The total momentum of the photoelectron is calculated from the measured kinetic energy

since the momentum of the electron parallel to the surface must be conserved, the original momentum of the electron can be computed from the polar angle of the sample to the detector and the azimuthal angle measured on the 2D detector

the perpendicular component of the original momentum can be obtained by assuming a free electron and measuring the inner potential, V_0 at $\theta = 0$

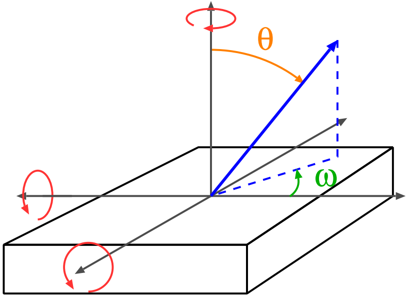

$$\hbar q_e = \sqrt{2m\mathcal{E}_{kin}}$$

$$\hbar q_{\|x} = \hbar q_e \sin\theta \cos\omega$$

$$\hbar q_{\|y} = \hbar q_e \sin\theta \sin\omega$$

Photoelectron momentum

The total momentum of the photoelectron is calculated from the measured kinetic energy

since the momentum of the electron parallel to the surface must be conserved, the original momentum of the electron can be computed from the polar angle of the sample to the detector and the azimuthal angle measured on the 2D detector

the perpendicular component of the original momentum can be obtained by assuming a free electron and measuring the inner potential, V_0 at $\theta = 0$

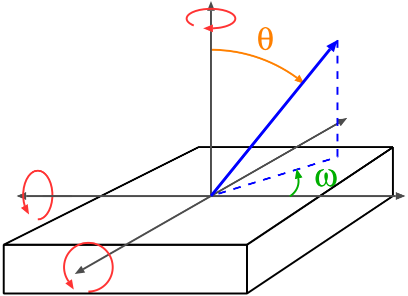

$$\hbar q_e = \sqrt{2m\mathcal{E}_{kin}}$$

$$\hbar q_{\|x} = \hbar q_e \sin\theta \cos\omega$$

$$\hbar q_{\|y} = \hbar q_e \sin\theta \sin\omega$$

$$\hbar q_{\perp} = \sqrt{2m(\mathcal{E}_{kin}\cos^2\theta + V_0)}$$

Photoelectron momentum

The total momentum of the photoelectron is calculated from the measured kinetic energy

since the momentum of the electron parallel to the surface must be conserved, the original momentum of the electron can be computed from the polar angle of the sample to the detector and the azimuthal angle measured on the 2D detector

the perpendicular component of the original momentum can be obtained by assuming a free electron and measuring the inner potential, V_0 at $\theta = 0$

the electron dispersion curve can be fully mapped by sample rotations

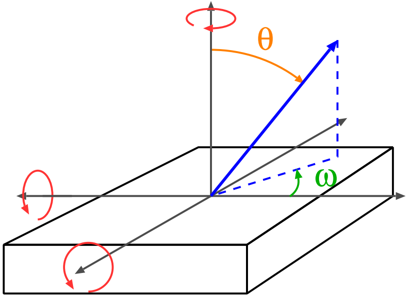

$$\hbar q_e = \sqrt{2m\mathcal{E}_{kin}}$$

$$\hbar q_{\|x} = \hbar q_e \sin\theta \cos\omega$$

$$\hbar q_{\|y} = \hbar q_e \sin\theta \sin\omega$$

$$\hbar q_{\perp} = \sqrt{2m(\mathcal{E}_{kin}\cos^2\theta + V_0)}$$

ARPES experimental data

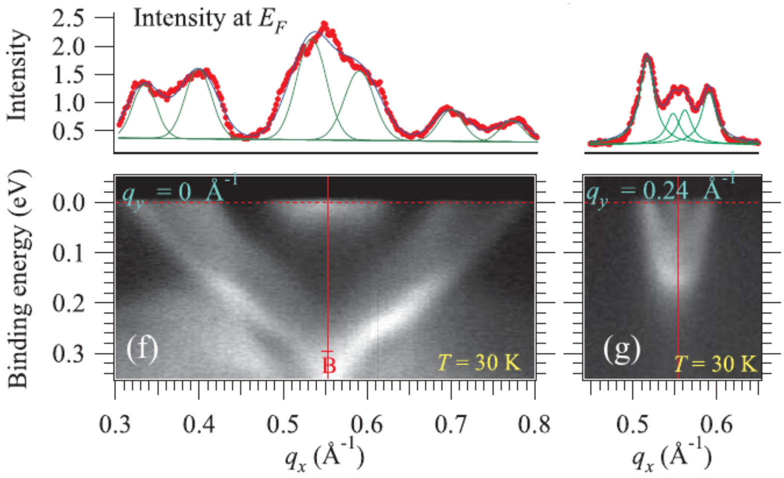

ARPES experimental data

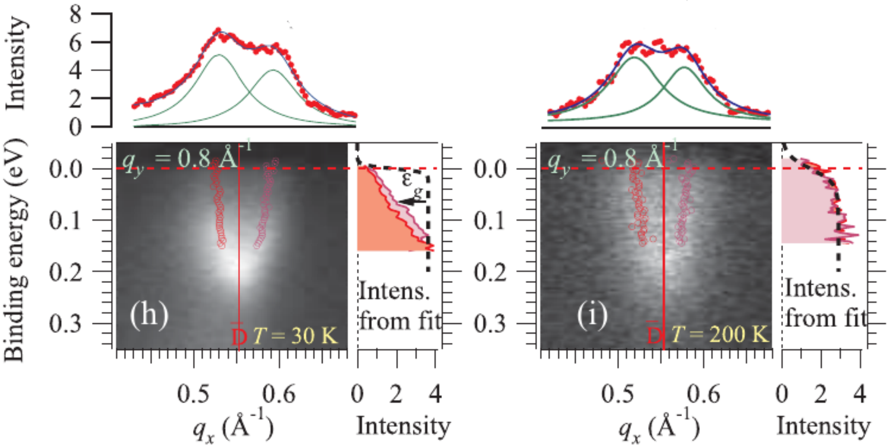

HAXPES

Photoemission spectroscopy is generally used for surface sensitive measurements because of the low energy of the incident photons (< 2 keV)

HAXPES

Photoemission spectroscopy is generally used for surface sensitive measurements because of the low energy of the incident photons (< 2 keV)

High energy synchrotrons offer the opportunity to use hard x-ray photoelectron spectroscopy (HAXPES)

HAXPES

Photoemission spectroscopy is generally used for surface sensitive measurements because of the low energy of the incident photons (< 2 keV)

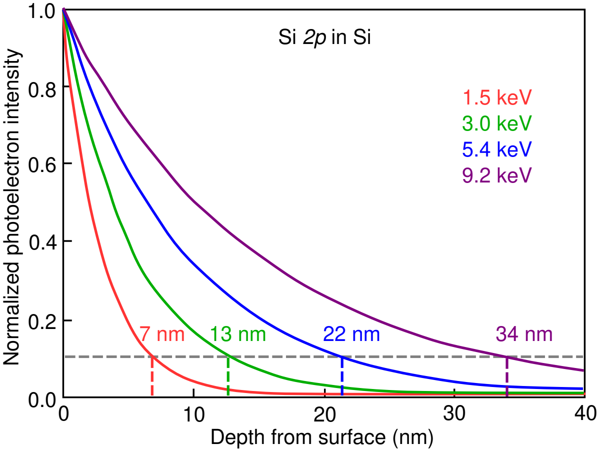

High energy synchrotrons offer the opportunity to use hard x-ray photoelectron spectroscopy (HAXPES)

HAXPES

Photoemission spectroscopy is generally used for surface sensitive measurements because of the low energy of the incident photons (< 2 keV)

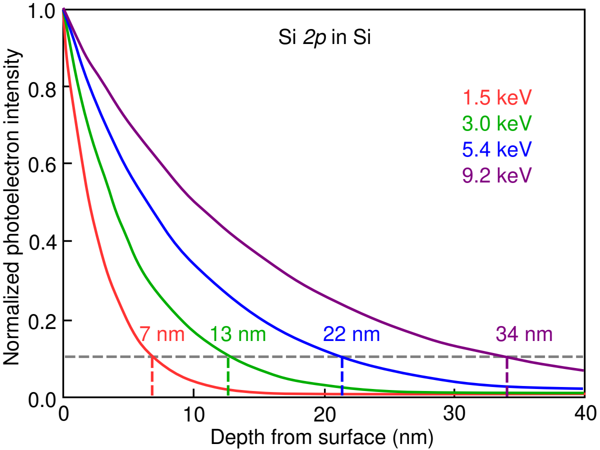

High energy synchrotrons offer the opportunity to use hard x-ray photoelectron spectroscopy (HAXPES)

HAXPES advantages include

HAXPES

Photoemission spectroscopy is generally used for surface sensitive measurements because of the low energy of the incident photons (< 2 keV)

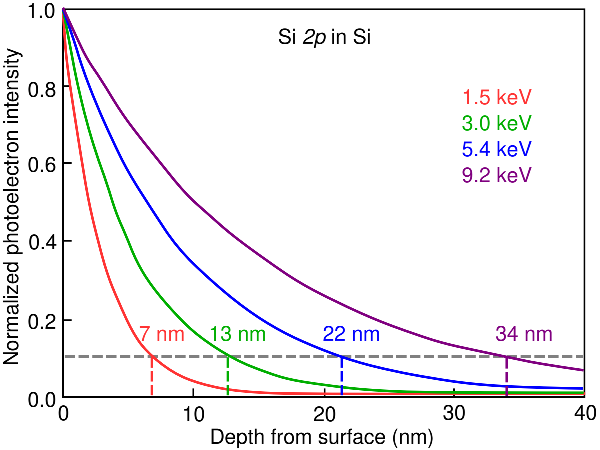

High energy synchrotrons offer the opportunity to use hard x-ray photoelectron spectroscopy (HAXPES)

HAXPES advantages include

measurement of K edges of 3d elements, L edges of 5d elements, and M edges of 5f elements

HAXPES

Photoemission spectroscopy is generally used for surface sensitive measurements because of the low energy of the incident photons (< 2 keV)

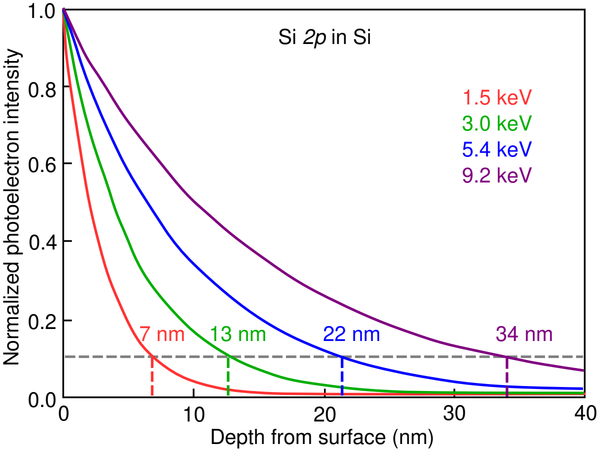

High energy synchrotrons offer the opportunity to use hard x-ray photo-electron spectroscopy (HAXPES)

HAXPES advantages include

measurement of K edges of 3d elements, L edges of 5d elements, and M edges of 5f elements

ability to measure bulk photoemission and buried interfaces as well as the surface

HAXPES of buried interfaces

HAXPES is used to probe the thickness of a $CoFe_2O_4/La_{0.66}Sr_{0.34}MnO_3$ heterostructure by varying both angle of incidence and photon energy

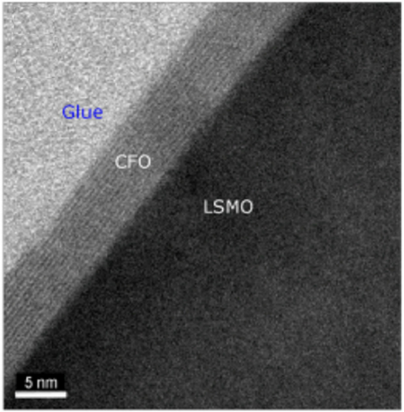

The thickness of the $CoFe_2O_4$ overlayer measured as 6.5 ± 0.5 nm by TEM was probed in two ways:

B. Pal, S. Mukherjee, and D.D. Sarma, "Probing complex heterostructures using hard x-ray photoelectron spectroscopy (HAXPES)," *J. Electron Spect. Related Phenomena* **200**, 332-339 (2015).

HAXPES of buried interfaces

HAXPES is used to probe the thickness of a $CoFe_2O_4/La_{0.66}Sr_{0.34}MnO_3$ heterostructure by varying both angle of incidence and photon energy

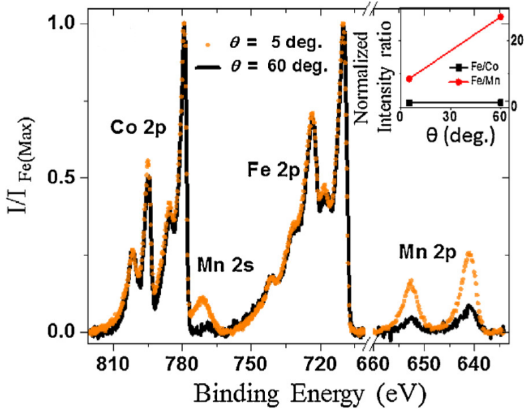

The thickness of the $CoFe_2O_4$ overlayer measured as 6.5 ± 0.5 nm by TEM was probed in two ways:

using 4.8 keV photons and varying the angle, the thickness is estimated to be 8.0 ± 2.0 nm

B. Pal, S. Mukherjee, and D.D. Sarma, "Probing complex heterostructures using hard x-ray photoelectron spectroscopy (HAXPES)," *J. Electron Spect. Related Phenomena* **200**, 332-339 (2015).

HAXPES of buried interfaces

HAXPES is used to probe the thickness of a $CoFe_2O_4/La_{0.66}Sr_{0.34}MnO_3$ heterostructure by varying both angle of incidence and photon energy

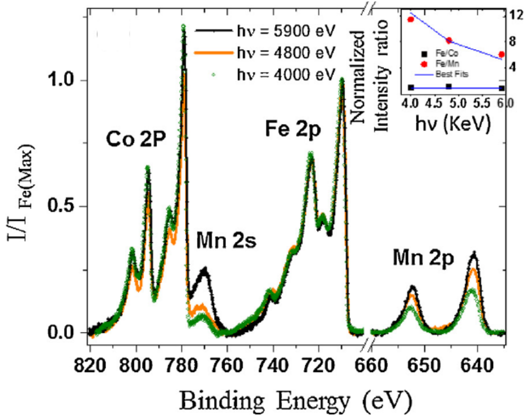

The thickness of the $CoFe_2O_4$ overlayer measured as 6.5 ± 0.5 nm by TEM was probed in two ways:

using 4.8 keV photons and varying the angle, the thickness is estimated to be 8.0 ± 2.0 nm

using photon energies from 4.0 keV to 6.0 keV, the thickness was estimated to be 6.8 ± 2.8 nm

B. Pal, S. Mukherjee, and D.D. Sarma, "Probing complex heterostructures using hard x-ray photoelectron spectroscopy (HAXPES)," *J. Electron Spect. Related Phenomena* **200**, 332-339 (2015).

HAXPES of buried interfaces

HAXPES is used to probe the thickness of a $CoFe_2O_4/La_{0.66}Sr_{0.34}MnO_3$ heterostructure by varying both angle of incidence and photon energy

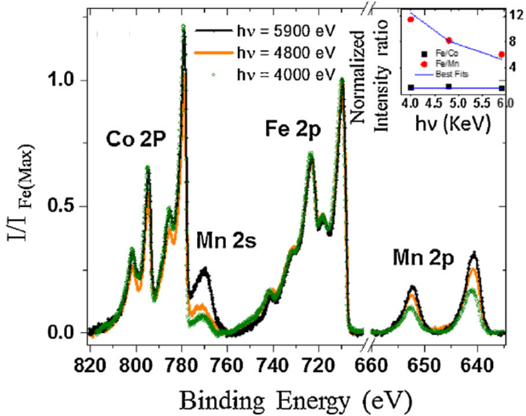

The thickness of the $CoFe_2O_4$ overlayer measured as 6.5 ± 0.5 nm by TEM was probed in two ways:

using 4.8 keV photons and varying the angle, the thickness is estimated to be 8.0 ± 2.0 nm

using photon energies from 4.0 keV to 6.0 keV, the thickness was estimated to be 6.8 ± 2.8 nm

Both results give consistent results with proper normalization and also show the uniformity of the $CoFe_2O_4$ overlayer

B. Pal, S. Mukherjee, and D.D. Sarma, "Probing complex heterostructures using hard x-ray photoelectron spectroscopy (HAXPES)," *J. Electron Spect. Related Phenomena* **200**, 332-339 (2015).

HAXPES of $Zn_{1-x}Cd_xSe_{1-y}S_y$ nanocrystals

Energy dispersive measurements can provide depth profiling of spherical nanoparticles

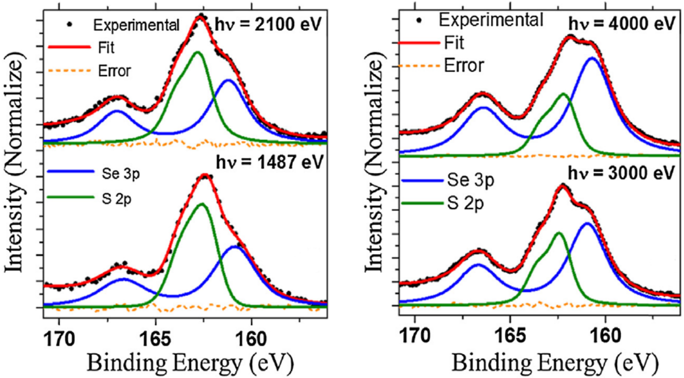

B. Pal, S. Mukherjee, and D.D. Sarma, "Probing complex heterostructures using hard x-ray photoelectron spectroscopy (HAXPES)," *J. Electron Spect. Related Phenomena* **200**, 332-339 (2015).

HAXPES of $Zn_{1-x}Cd_xSe_{1-y}S_y$ nanocrystals

Energy dispersive measurements can provide depth profiling of spherical nanoparticles

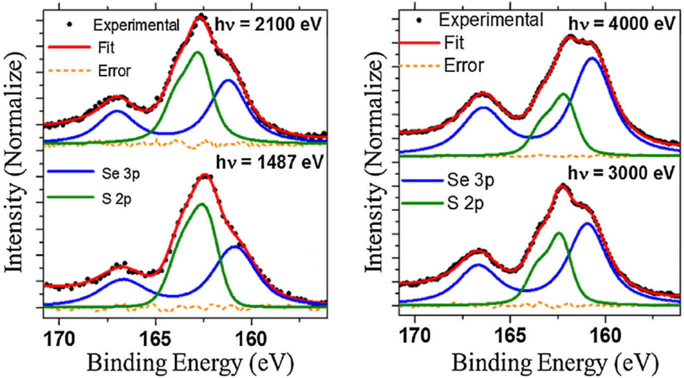

HAXPES at energies ranging from 1.4 keV to 3.0 keV are used to probe the S/Se ratio at varying depths of the 5 nm diameter nanoparticles

B. Pal, S. Mukherjee, and D.D. Sarma, "Probing complex heterostructures using hard x-ray photoelectron spectroscopy (HAXPES)," *J. Electron Spect. Related Phenomena* **200**, 332-339 (2015).

HAXPES of $Zn_{1-x}Cd_xSe_{1-y}S_y$ nanocrystals

Energy dispersive measurements can provide depth profiling of spherical nanoparticles

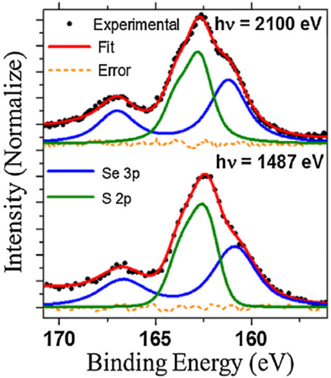

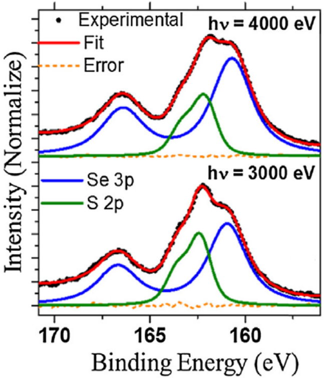

HAXPES at energies ranging from 1.4 keV to 3.0 keV are used to probe the S/Se ratio at varying depths of the 5 nm diameter nanoparticles

By fitting the S 2*p* and Se 3*p* photoemission line the structure is revealed to be CdSe at the core and ZnCdS in the outer shell

B. Pal, S. Mukherjee, and D.D. Sarma, "Probing complex heterostructures using hard x-ray photoelectron spectroscopy (HAXPES)," *J. Electron Spect. Related Phenomena* **200**, 332-339 (2015).

HAXPES of $Zn_{1-x}Cd_xSe_{1-y}S_y$ nanocrystals

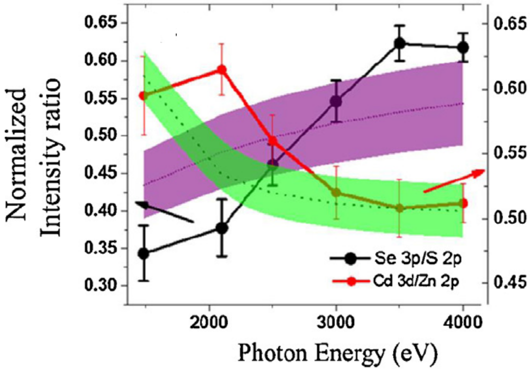

The variation in intensity of the Se/S lines and the Zn/Cd lines suggest that the Se is primarily located in the 2 nm core of the 5 nm particles with the Cd

B. Pal, S. Mukherjee, and D.D. Sarma, "Probing complex heterostructures using hard x-ray photoelectron spectroscopy (HAXPES)," *J. Electron Spect. Related Phenomena* **200**, 332-339 (2015).

HAXPES of $Zn_{1-x}Cd_xSe_{1-y}S_y$ nanocrystals

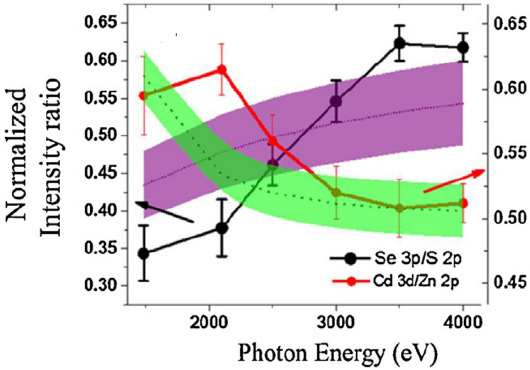

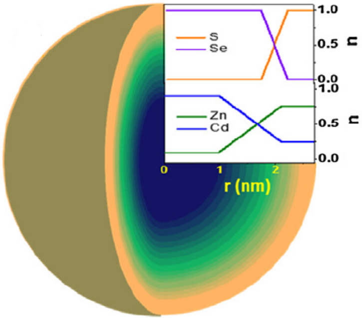

The variation in intensity of the Se/S lines and the Zn/Cd lines suggest that the Se is primarily located in the 2 nm core of the 5 nm particles with the Cd and that there is a graded composition region between the CdSe core and the outer ZnCdS shell

B. Pal, S. Mukherjee, and D.D. Sarma, "Probing complex heterostructures using hard x-ray photoelectron spectroscopy (HAXPES)," *J. Electron Spect. Related Phenomena* **200**, 332-339 (2015).

HAXPES of Si anodes

Si nanoparticle anodes suffer from the accumulation of the SEI layer which reduces performance. The SEI is formed by electrochemical decomposition of the electrolyte at the anode surface.

B.T. Young, et al., "Hard x-ray photoelectron spectroscopy (HAXPES) investigation of the silicon solid electrolyte interphase (SEI) in lithium-ion batteries," *ACS Appl. Mater. Interfaces* **7**, 20004-20011 (2015).

HAXPES of Si anodes

Si nanoparticle anodes suffer from the accumulation of the SEI layer which reduces performance. The SEI is formed by electrochemical decomposition of the electrolyte at the anode surface.

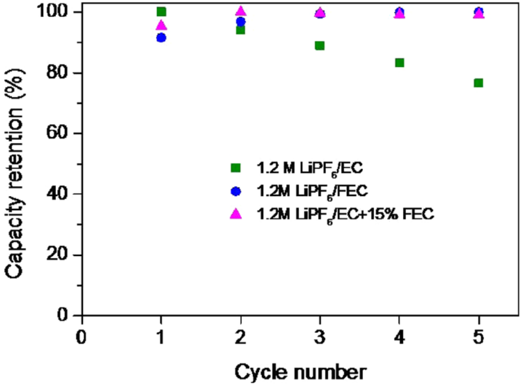

B.T. Young, et al., "Hard x-ray photoelectron spectroscopy (HAXPES) investigation of the silicon solid electrolyte interphase (SEI) in lithium-ion batteries," *ACS Appl. Mater. Interfaces* **7**, 20004-20011 (2015).

HAXPES of Si anodes

Si nanoparticle anodes suffer from the accumulation of the SEI layer which reduces performance. The SEI is formed by electrochemical decomposition of the electrolyte at the anode surface.

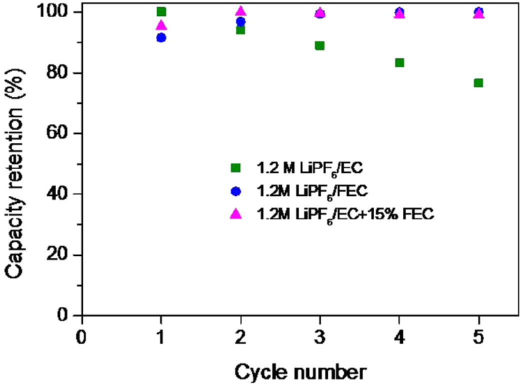

The SEI from three different electrolyte combinations were studied: ethylene carbonate (EC), fluoroethylene carbonate (FEC), and a combination. The first of which gives poorer capacity and cycling stability.

B.T. Young, et al., "Hard x-ray photoelectron spectroscopy (HAXPES) investigation of the silicon solid electrolyte interphase (SEI) in lithium-ion batteries," *ACS Appl. Mater. Interfaces* **7**, 20004-20011 (2015).

HAXPES of Si anodes

Si nanoparticle anodes suffer from the accumulation of the SEI layer which reduces performance. The SEI is formed by electrochemical decomposition of the electrolyte at the anode surface.

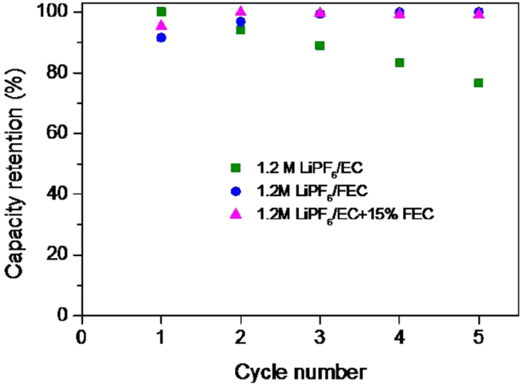

The SEI from three different electrolyte combinations were studied: ethylene carbonate (EC), fluoroethylene carbonate (FEC), and a combination. The first of which gives poorer capacity and cycling stability.

HAXPES is used to determine the elemental distribution and compounds present as a function of depth in the cycled Si anode.

B.T. Young, et al., "Hard x-ray photoelectron spectroscopy (HAXPES) investigation of the silicon solid electrolyte interphase (SEI) in lithium-ion batteries," *ACS Appl. Mater. Interfaces* **7**, 20004-20011 (2015).

HAXPES of Si anodes

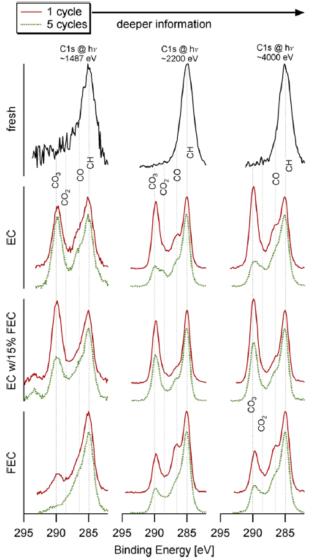

By varying the incident photon energy, it is possible to probe the SEI as a function of depth.

B.T. Young, et al., "Hard x-ray photoelectron spectroscopy (HAXPES) investigation of the silicon solid electrolyte interphase (SEI) in lithium-ion batteries," *ACS Appl. Mater. Interfaces* **7**, 20004-20011 (2015).

HAXPES of Si anodes

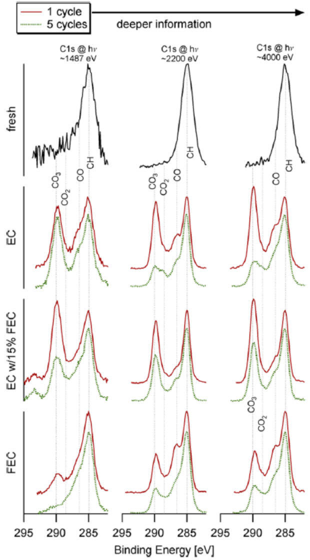

By varying the incident photon energy, it is possible to probe the SEI as a function of depth.

From the carbon peaks, it is seen that:

B.T. Young, et al., "Hard x-ray photoelectron spectroscopy (HAXPES) investigation of the silicon solid electrolyte interphase (SEI) in lithium-ion batteries," *ACS Appl. Mater. Interfaces* **7**, 20004-20011 (2015).

HAXPES of Si anodes

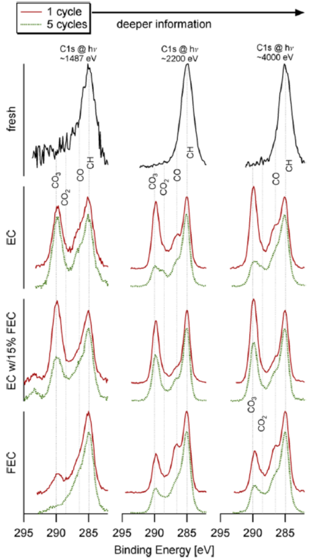

By varying the incident photon energy, it is possible to probe the SEI as a function of depth.

From the carbon peaks, it is seen that:

- increase in carbon concentration is SEI

B.T. Young, et al., "Hard x-ray photoelectron spectroscopy (HAXPES) investigation of the silicon solid electrolyte interphase (SEI) in lithium-ion batteries," *ACS Appl. Mater. Interfaces* **7**, 20004-20011 (2015).

HAXPES of Si anodes

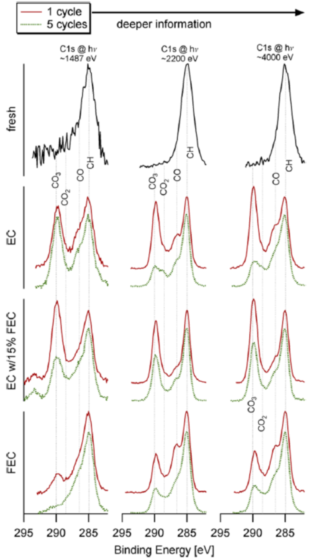

By varying the incident photon energy, it is possible to probe the SEI as a function of depth.

From the carbon peaks, it is seen that:

- increase in carbon concentration is SEI
- SEI visible after first cycle with EC is likely lithium ethylene dicarbonate (LEDC, 290 eV peak)

B.T. Young, et al., "Hard x-ray photoelectron spectroscopy (HAXPES) investigation of the silicon solid electrolyte interphase (SEI) in lithium-ion batteries," *ACS Appl. Mater. Interfaces* **7**, 20004-20011 (2015).

HAXPES of Si anodes

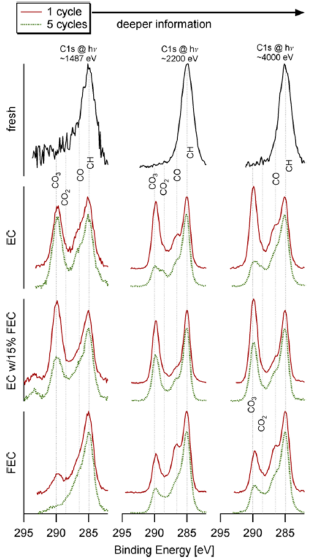

By varying the incident photon energy, it is possible to probe the SEI as a function of depth.

From the carbon peaks, it is seen that:

- increase in carbon concentration is SEI
- SEI visible after first cycle with EC is likely lithium ethylene dicarbonate (LEDC, 290 eV peak)
- after 5 cycles, buried LEDC decomposes in EC electrolytes

B.T. Young, et al., "Hard x-ray photoelectron spectroscopy (HAXPES) investigation of the silicon solid electrolyte interphase (SEI) in lithium-ion batteries," *ACS Appl. Mater. Interfaces* **7**, 20004-20011 (2015).

HAXPES of Si anodes

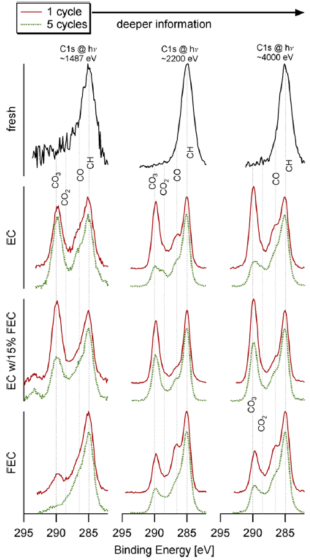

By varying the incident photon energy, it is possible to probe the SEI as a function of depth.

From the carbon peaks, it is seen that:

- increase in carbon concentration is SEI
- SEI visible after first cycle with EC is likely lithium ethylene dicarbonate (LEDC, 290 eV peak)
- after 5 cycles, buried LEDC decomposes in EC electrolytes
- pure FEC shows little LEDC

B.T. Young, et al., "Hard x-ray photoelectron spectroscopy (HAXPES) investigation of the silicon solid electrolyte interphase (SEI) in lithium-ion batteries," *ACS Appl. Mater. Interfaces* **7**, 20004-20011 (2015).

HAXPES of Si anodes

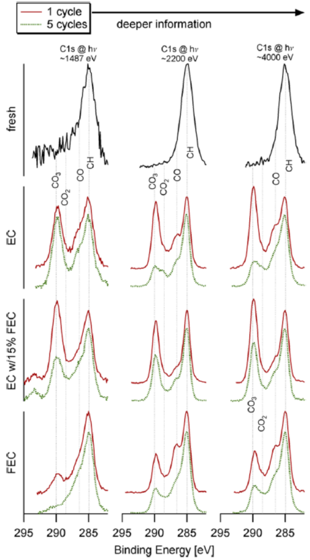

By varying the incident photon energy, it is possible to probe the SEI as a function of depth.

From the carbon peaks, it is seen that:

- increase in carbon concentration is SEI
- SEI visible after first cycle with EC is likely lithium ethylene dicarbonate (LEDC, 290 eV peak)
- after 5 cycles, buried LEDC decomposes in EC electrolytes
- pure FEC shows little LEDC
- pure FEC shows less change with cycling than EC containing electrolytes

B.T. Young, et al., “Hard x-ray photoelectron spectroscopy (HAXPES) investigation of the silicon solid electrolyte interphase (SEI) in lithium-ion batteries,” *ACS Appl. Mater. Interfaces* **7**, 20004-20011 (2015).

HAXPES of Si anodes

Using HAXPES data from Si, C, and F, a picture of SEI evolution dependence on electrolyte emerges

B.T. Young, et al., "Hard x-ray photoelectron spectroscopy (HAXPES) investigation of the silicon solid electrolyte interphase (SEI) in lithium-ion batteries," *ACS Appl. Mater. Interfaces* **7**, 20004-20011 (2015).

HAXPES of Si anodes

Using HAXPES data from Si, C, and F, a picture of SEI evolution dependence on electrolyte emerges

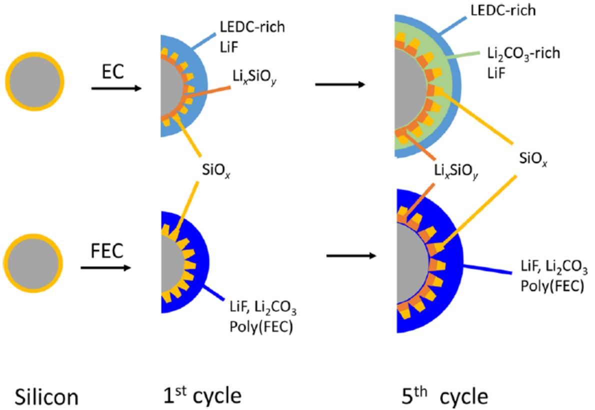

B.T. Young, et al., "Hard x-ray photoelectron spectroscopy (HAXPES) investigation of the silicon solid electrolyte interphase (SEI) in lithium-ion batteries," *ACS Appl. Mater. Interfaces* **7**, 20004-20011 (2015).

HAXPES of Si anodes

Using HAXPES data from Si, C, and F, a picture of SEI evolution dependence on electrolyte emerges

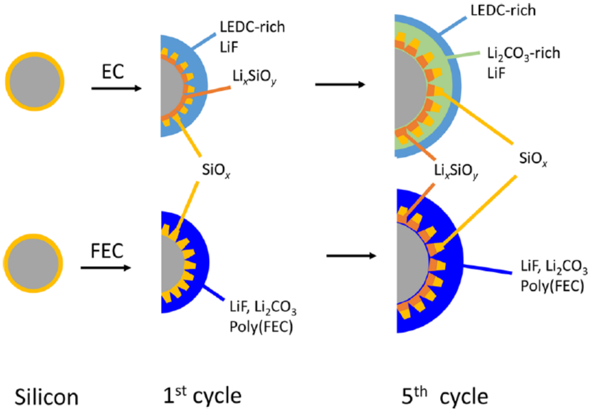

as SEI grows, there is growth of Li_xSiO_y underneath as product of lithiation/delithiation

B.T. Young, et al., "Hard x-ray photoelectron spectroscopy (HAXPES) investigation of the silicon solid electrolyte interphase (SEI) in lithium-ion batteries," *ACS Appl. Mater. Interfaces* **7**, 20004-20011 (2015).

HAXPES of Si anodes

Using HAXPES data from Si, C, and F, a picture of SEI evolution dependence on electrolyte emerges

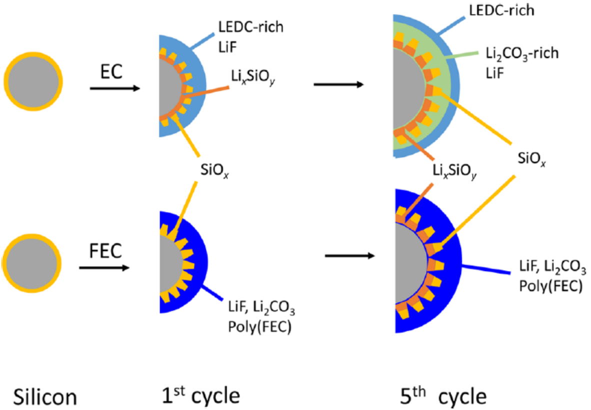

as SEI grows, there is growth of Li_xSiO_y underneath as product of lithiation/delithiation

EC – SEI contains LEDC-rich SEI which decomposes but continues be deposited with cycling

B.T. Young, et al., "Hard x-ray photoelectron spectroscopy (HAXPES) investigation of the silicon solid electrolyte interphase (SEI) in lithium-ion batteries," *ACS Appl. Mater. Interfaces* **7**, 20004-20011 (2015).

HAXPES of Si anodes

Using HAXPES data from Si, C, and F, a picture of SEI evolution dependence on electrolyte emerges

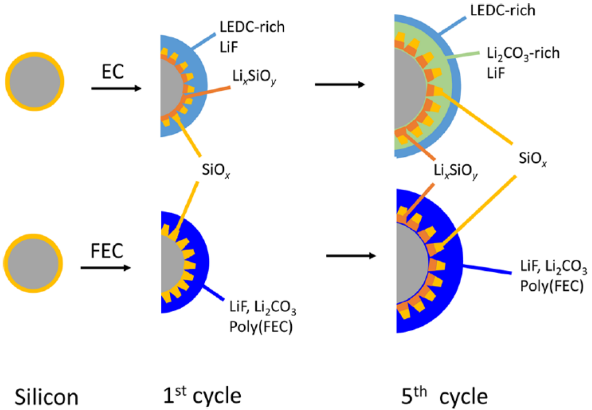

as SEI grows, there is growth of Li_xSiO_y underneath as product of lithiation/delithiation

EC – SEI contains LEDC-rich SEI which decomposes but continues be deposited with cycling

FEC – SEI is mostly poly-FEC with LiF and $LiCO_3$ which remains stable with cycling

B.T. Young, et al., "Hard x-ray photoelectron spectroscopy (HAXPES) investigation of the silicon solid electrolyte interphase (SEI) in lithium-ion batteries," *ACS Appl. Mater. Interfaces* **7**, 20004-20011 (2015).

HAXPES of Si anodes

Using HAXPES data from Si, C, and F, a picture of SEI evolution dependence on electrolyte emerges

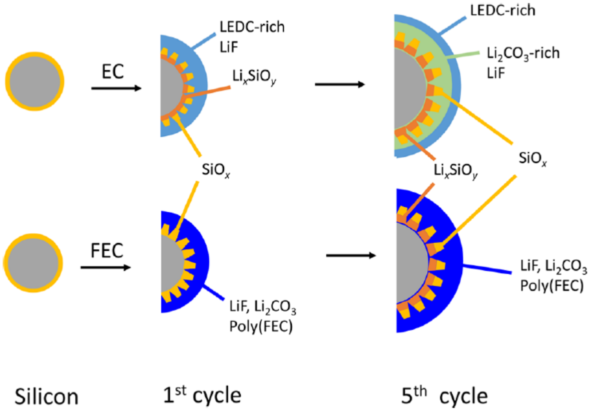

as SEI grows, there is growth of Li_xSiO_y underneath as product of lithiation/delithiation

EC – SEI contains LEDC-rich SEI which decomposes but continues be deposited with cycling

FEC – SEI is mostly poly-FEC with LiF and $LiCO_3$ which remains stable with cycling

The FEC acts to stabilize the SEI composition and prevent the change with depth that occurs with EC.

B.T. Young, et al., "Hard x-ray photoelectron spectroscopy (HAXPES) investigation of the silicon solid electrolyte interphase (SEI) in lithium-ion batteries," *ACS Appl. Mater. Interfaces* **7**, 20004-20011 (2015).

X-ray magnetic circular dichroism

The interaction x-rays with magnetic systems is generally weak and not considered in scattering experiments

X-ray magnetic circular dichroism

The interaction x-rays with magnetic systems is generally weak and not considered in scattering experiments

One exception is the absorption coefficient of circularly polarized x-rays

X-ray magnetic circular dichroism

The interaction x-rays with magnetic systems is generally weak and not considered in scattering experiments

One exception is the absorption coefficient of circularly polarized x-rays

in a normal x-ray absorption event, the selection rules for a transition are $\Delta l = \pm 1$, $\Delta m = 0, \pm 1$

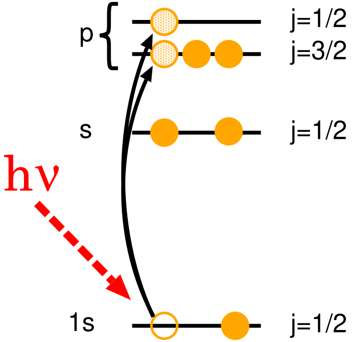

X-ray magnetic circular dichroism

The interaction x-rays with magnetic systems is generally weak and not considered in scattering experiments

One exception is the absorption coefficient of circularly polarized x-rays

in a normal x-ray absorption event, the selection rules for a transition are $\Delta l = \pm 1$, $\Delta m = 0, \pm 1$

if circularly polarized x-rays are used, however, the selection rules for m depend on the "handedness" of the radiation

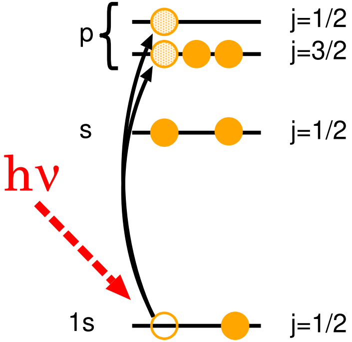

X-ray magnetic circular dichroism

The interaction x-rays with magnetic systems is generally weak and not considered in scattering experiments

One exception is the absorption coefficient of circularly polarized x-rays

in a normal x-ray absorption event, the selection rules for a transition are $\Delta l = \pm 1$, $\Delta m = 0, \pm 1$

if circularly polarized x-rays are used, however, the selection rules for m depend on the "handedness" of the radiation

$\Delta m = +1$ for "right-handed"

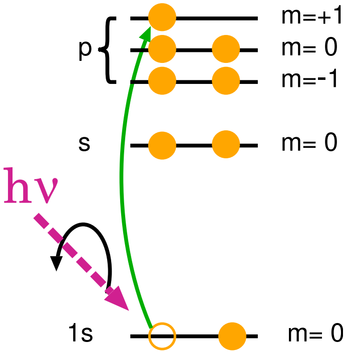

X-ray magnetic circular dichroism

The interaction x-rays with magnetic systems is generally weak and not considered in scattering experiments

One exception is the absorption coefficient of circularly polarized x-rays

in a normal x-ray absorption event, the selection rules for a transition are $\Delta l = \pm 1$, $\Delta m = 0, \pm 1$

if circularly polarized x-rays are used, however, the selection rules for m depend on the "handedness" of the radiation

$\Delta m = +1$ for "right-handed"

$\Delta m = -1$ for "left-handed"

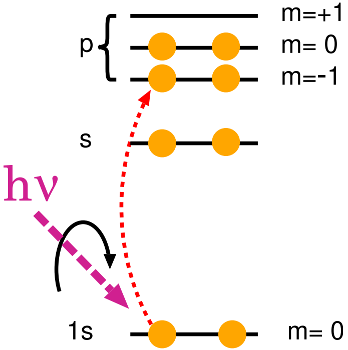

X-ray magnetic circular dichroism

The interaction x-rays with magnetic systems is generally weak and not considered in scattering experiments

One exception is the absorption coefficient of circularly polarized x-rays

in a normal x-ray absorption event, the selection rules for a transition are $\Delta l = \pm 1$, $\Delta m = 0, \pm 1$

if circularly polarized x-rays are used, however, the selection rules for m depend on the "handedness" of the radiation

$\Delta m = +1$ for "right-handed"

$\Delta m = -1$ for "left-handed"

this measurement is sensitive to the internal/external magnetic fields which split the levels according to the Zeeman effect

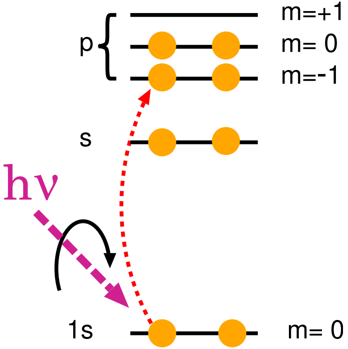

XMCD and electron sum rules

The XMCD experiment requires a source capable of switching the polarization (quarter wave plate) or a sample whose magnetic splittings can be inverted by flipping an external magnetic field

XMCD and electron sum rules

The XMCD experiment requires a source capable of switching the polarization (quarter wave plate) or a sample whose magnetic splittings can be inverted by flipping an external magnetic field

The absorption coefficient is first measured for both relative orientations of magnetic splitting and circular polarization

XMCD and electron sum rules

The XMCD experiment requires a source capable of switching the polarization (quarter wave plate) or a sample whose magnetic splittings can be inverted by flipping an external magnetic field

The absorption coefficient is first measured for both relative orientations of magnetic splitting and circular polarization

$$\mu^+(\mathcal{E}) = \frac{1}{x} \ln \left(\frac{I_0^+}{I_t^+} \right)$$

XMCD and electron sum rules

The XMCD experiment requires a source capable of switching the polarization (quarter wave plate) or a sample whose magnetic splittings can be inverted by flipping an external magnetic field

The absorption coefficient is first measured for both relative orientations of magnetic splitting and circular polarization

$$\mu^{+}(\mathcal{E}) = \frac{1}{x} \ln\left(\frac{I_0^{+}}{I_t^{+}}\right)$$

$$\mu^{-}(\mathcal{E}) = \frac{1}{x} \ln\left(\frac{I_0^{-}}{I_t^{-}}\right)$$

XMCD and electron sum rules

The XMCD experiment requires a source capable of switching the polarization (quarter wave plate) or a sample whose magnetic splittings can be inverted by flipping an external magnetic field

The absorption coefficient is first measured for both relative orientations of magnetic splitting and circular polarization

$$\mu^+(\mathcal{E}) = \frac{1}{x} \ln\left(\frac{I_0^+}{I_t^+}\right)$$

$$\mu^-(\mathcal{E}) = \frac{1}{x} \ln\left(\frac{I_0^-}{I_t^-}\right)$$

these absorption coefficients can be used at the L_3 and L_2 edges to compute the orbital (m_{orb}) and spin (m_{spin}) magnetic moments in μ_B/atom

XMCD and electron sum rules

The XMCD experiment requires a source capable of switching the polarization (quarter wave plate) or a sample whose magnetic splittings can be inverted by flipping an external magnetic field

The absorption coefficient is first measured for both relative orientations of magnetic splitting and circular polarization

$$\mu^{+}(\mathcal{E}) = \frac{1}{x}\ln\left(\frac{I_0^{+}}{I_t^{+}}\right)$$

$$\mu^{-}(\mathcal{E}) = \frac{1}{x}\ln\left(\frac{I_0^{-}}{I_t^{-}}\right)$$

these absorption coefficients can be used at the L_3 and L_2 edges to compute the orbital (m_{orb}) and spin (m_{spin}) magnetic moments in μ_B/atom

$$m_{orb} = -\frac{4q(10 - n_{3d})}{r}$$

XMCD and electron sum rules

The XMCD experiment requires a source capable of switching the polarization (quarter wave plate) or a sample whose magnetic splittings can be inverted by flipping an external magnetic field

The absorption coefficient is first measured for both relative orientations of magnetic splitting and circular polarization

$$\mu^{+}(\mathcal{E}) = \frac{1}{x} \ln\left(\frac{I_0^{+}}{I_t^{+}}\right)$$

$$\mu^{-}(\mathcal{E}) = \frac{1}{x} \ln\left(\frac{I_0^{-}}{I_t^{-}}\right)$$

these absorption coefficients can be used at the L_3 and L_2 edges to compute the orbital (m_{orb}) and spin (m_{spin}) magnetic moments in μ_B/atom

$$m_{orb} = -\frac{4q(10 - n_{3d})}{r}$$

$$m_{spin} \approx -\frac{(6p - 4q)(10 - n_{3d})}{r}$$

XMCD and electron sum rules

The XMCD experiment requires a source capable of switching the polarization (quarter wave plate) or a sample whose magnetic splittings can be inverted by flipping an external magnetic field

The absorption coefficient is first measured for both relative orientations of magnetic splitting and circular polarization

$$\mu^+(\mathcal{E}) = \frac{1}{x} \ln\left(\frac{I_0^+}{I_t^+}\right)$$

$$\mu^-(\mathcal{E}) = \frac{1}{x} \ln\left(\frac{I_0^-}{I_t^-}\right)$$

these absorption coefficients can be used at the L_3 and L_2 edges to compute the orbital (m_{orb}) and spin (m_{spin}) magnetic moments in μ_B/atom

$$p = \int_{L_3} (\mu^+ - \mu^-) d\mathcal{E}$$

$$m_{orb} = -\frac{4q(10 - n_{3d})}{r}$$

$$m_{spin} \approx -\frac{(6p - 4q)(10 - n_{3d})}{r}$$

XMCD and electron sum rules

The XMCD experiment requires a source capable of switching the polarization (quarter wave plate) or a sample whose magnetic splittings can be inverted by flipping an external magnetic field

The absorption coefficient is first measured for both relative orientations of magnetic splitting and circular polarization

$$\mu^+(\mathcal{E}) = \frac{1}{x} \ln\left(\frac{I_0^+}{I_t^+}\right)$$

$$\mu^-(\mathcal{E}) = \frac{1}{x} \ln\left(\frac{I_0^-}{I_t^-}\right)$$

these absorption coefficients can be used at the L_3 and L_2 edges to compute the orbital (m_{orb}) and spin (m_{spin}) magnetic moments in μ_B/atom

$$p = \int_{L_3} (\mu^+ - \mu^-) d\mathcal{E}$$

$$q = \int_{L_3+L_2} (\mu^+ - \mu^-) d\mathcal{E}$$

$$m_{orb} = -\frac{4q(10 - n_{3d})}{r}$$

$$m_{spin} \approx -\frac{(6p - 4q)(10 - n_{3d})}{r}$$

XMCD and electron sum rules

The XMCD experiment requires a source capable of switching the polarization (quarter wave plate) or a sample whose magnetic splittings can be inverted by flipping an external magnetic field

The absorption coefficient is first measured for both relative orientations of magnetic splitting and circular polarization

$$\mu^+(\mathcal{E}) = \frac{1}{x} \ln\left(\frac{I_0^+}{I_t^+}\right)$$

$$\mu^-(\mathcal{E}) = \frac{1}{x} \ln\left(\frac{I_0^-}{I_t^-}\right)$$

these absorption coefficients can be used at the L_3 and L_2 edges to compute the orbital (m_{orb}) and spin (m_{spin}) magnetic moments in μ_B/atom

$$p = \int_{L_3} (\mu^+ - \mu^-) d\mathcal{E}$$

$$q = \int_{L_3+L_2} (\mu^+ - \mu^-) d\mathcal{E}$$

$$r = \int_{L_3+L_2} (\mu^+ + \mu^-) d\mathcal{E}$$

$$m_{orb} = -\frac{4q(10 - n_{3d})}{r}$$

$$m_{spin} \approx -\frac{(6p - 4q)(10 - n_{3d})}{r}$$

XMCD of $Yb_{14}MnSb_{11}$

The Zintl compounds exhibit interesting magnetic properties including colossal magnetoresistance which can be of value for spintronics applications

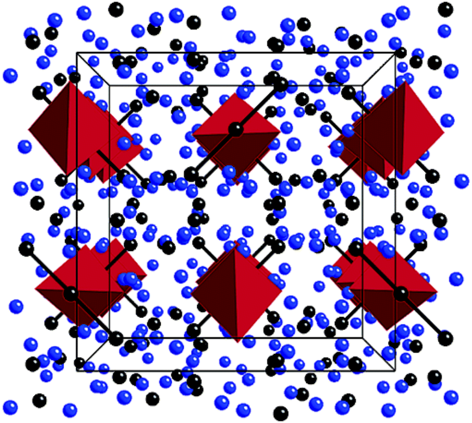

"XMCD Characterization of the Ferromagnetic State of $Yb_{14}MnSb_{11}$," A.P. Holm, S.M. Kauzlarich, S.A. Morton, G.D. Waddill, W.E. Pickett, and J.G. Tobin, *J. Am. Chem. Soc.* **124**, 9894-9898 (2002).

XMCD of $Yb_{14}MnSb_{11}$

The Zintl compounds exhibit interesting magnetic properties including colossal magnetoresistance which can be of value for spintronics applications

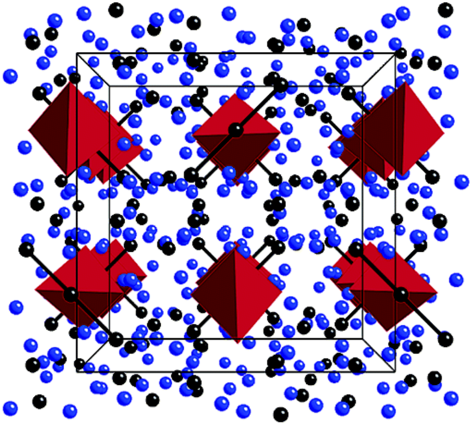

The Zintl compound, $Yb_{14}MnSb_{11}$ is ferromagnetic below below 56K with a moment of $\sim 4\mu_B$/formula unit

"XMCD Characterization of the Ferromagnetic State of $Yb_{14}MnSb_{11}$," A.P. Holm, S.M. Kauzlarich, S.A. Morton, G.D. Waddill, W.E. Pickett, and J.G. Tobin, *J. Am. Chem. Soc.* **124**, 9894-9898 (2002).

XMCD of $Yb_{14}MnSb_{11}$

The Zintl compounds exhibit interesting magnetic properties including colossal magnetoresistance which can be of value for spintronics applications

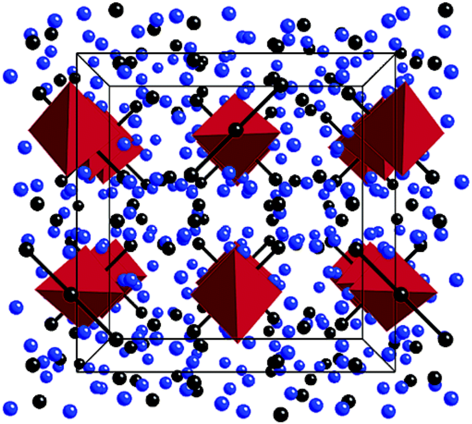

The Zintl compound, $Yb_{14}MnSb_{11}$ is ferromagnetic below below 56K with a moment of $\sim 4\mu_B$/formula unit

The Mn atom is in a tetrahedral environment surrounded by 4 Sb atoms and there are linear chains of Sb (black) atoms surrounded by Yb (blue) atoms

"XMCD Characterization of the Ferromagnetic State of $Yb_{14}MnSb_{11}$," A.P. Holm, S.M. Kauzlarich, S.A. Morton, G.D. Waddill, W.E. Pickett, and J.G. Tobin, *J. Am. Chem. Soc.* **124**, 9894-9898 (2002).

XMCD of $Yb_{14}MnSb_{11}$

The Zintl compounds exhibit interesting magnetic properties including colossal magnetoresistance which can be of value for spintronics applications

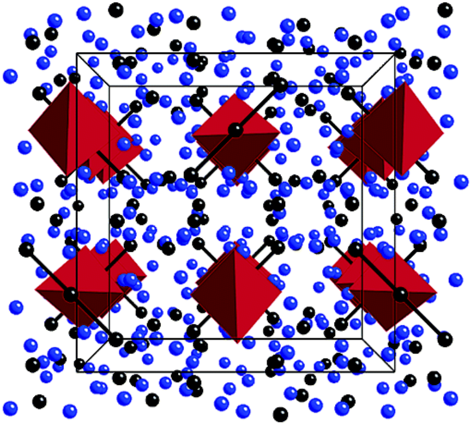

The Zintl compound, $Yb_{14}MnSb_{11}$ is ferromagnetic below below 56K with a moment of $\sim 4\mu_B$/formula unit

The Mn atom is in a tetrahedral environment surrounded by 4 Sb atoms and there are linear chains of Sb (black) atoms surrounded by Yb (blue) atoms

XMCD on a single crystal of $Yb_{14}MnSb_{11}$ can be used to understand the origin of the ferromagnetic moment

"XMCD Characterization of the Ferromagnetic State of $Yb_{14}MnSb_{11}$," A.P. Holm, S.M. Kauzlarich, S.A. Morton, G.D. Waddill, W.E. Pickett, and J.G. Tobin, *J. Am. Chem. Soc.* **124**, 9894-9898 (2002).

XMCD of $Yb_{14}MnSb_{11}$

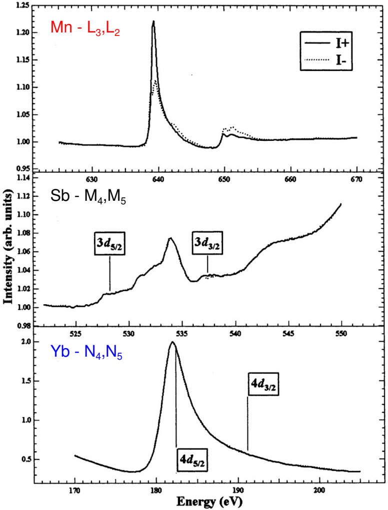

"XMCD Characterization of the Ferromagnetic State of $Yb_{14}MnSb_{11}$," A.P. Holm, S.M. Kauzlarich, S.A. Morton, G.D. Waddill, W.E. Pickett, and J.G. Tobin, *J. Am. Chem. Soc.* **124**, 9894-9898 (2002).

XMCD of $Yb_{14}MnSb_{11}$

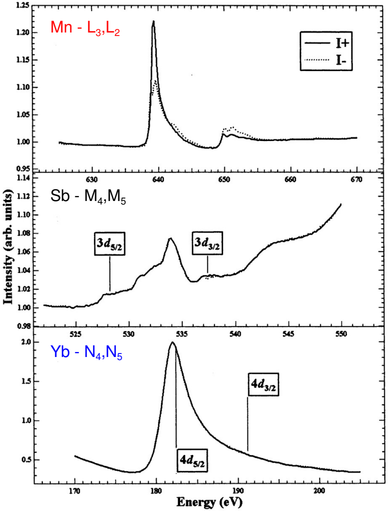

The Yb XMCD shows no asymmetry due to polarization

"XMCD Characterization of the Ferromagnetic State of $Yb_{14}MnSb_{11}$," A.P. Holm, S.M. Kauzlarich, S.A. Morton, G.D. Waddill, W.E. Pickett, and J.G. Tobin, *J. Am. Chem. Soc.* **124**, 9894-9898 (2002).

XMCD of $Yb_{14}MnSb_{11}$

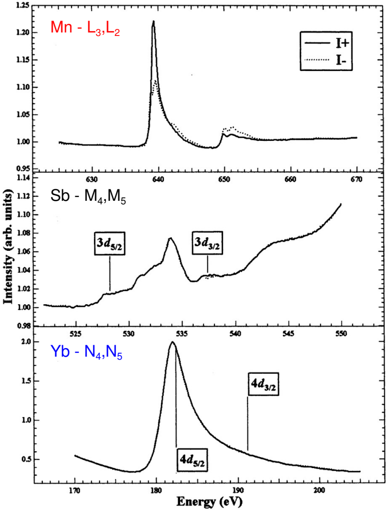

The Yb XMCD shows no asymmetry due to polarization

The Mn spectrum shows a significant asymmetry in opposite directions for the L_3 and L_2 edges

"XMCD Characterization of the Ferromagnetic State of $Yb_{14}MnSb_{11}$," A.P. Holm, S.M. Kauzlarich, S.A. Morton, G.D. Waddill, W.E. Pickett, and J.G. Tobin, *J. Am. Chem. Soc.* **124**, 9894-9898 (2002).

XMCD of $Yb_{14}MnSb_{11}$

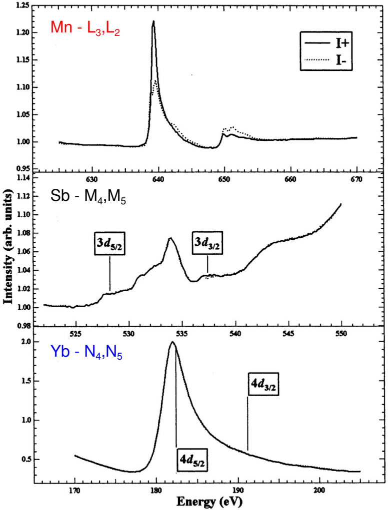

The Yb XMCD shows no asymmetry due to polarization

The Mn spectrum shows a significant asymmetry in opposite directions for the L_3 and L_2 edges

The Sb edges show a tiny asymmetry that is in opposite sign compared to the Mn edges

"XMCD Characterization of the Ferromagnetic State of $Yb_{14}MnSb_{11}$," A.P. Holm, S.M. Kauzlarich, S.A. Morton, G.D. Waddill, W.E. Pickett, and J.G. Tobin, *J. Am. Chem. Soc.* **124**, 9894-9898 (2002).

XMCD of $Yb_{14}MnSb_{11}$

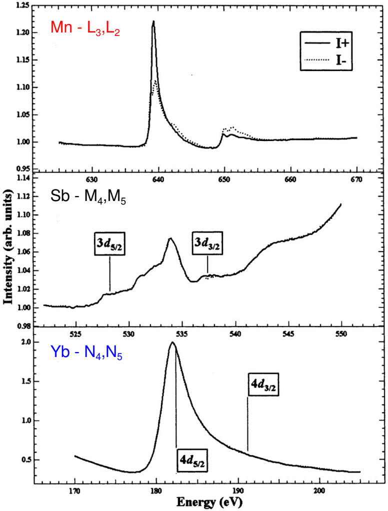

The Yb XMCD shows no asymmetry due to polarization

The Mn spectrum shows a significant asymmetry in opposite directions for the L_3 and L_2 edges

The Sb edges show a tiny asymmetry that is in opposite sign compared to the Mn edges

Mn provides the bulk of the magnetic moment and appears to be in the divalent state. Sb provides a small antiferromagnetic component to the overall magnetic moment

"XMCD Characterization of the Ferromagnetic State of $Yb_{14}MnSb_{11}$," A.P. Holm, S.M. Kauzlarich, S.A. Morton, G.D. Waddill, W.E. Pickett, and J.G. Tobin, *J. Am. Chem. Soc.* **124**, 9894-9898 (2002).

A better scattering model

Up to now, scattering has been treated classically and the result of radiation interaction with "free" electrons.

A better scattering model

Up to now, scattering has been treated classically and the result of radiation interaction with "free" electrons.

This is not a good approximation since we know:

A better scattering model

Up to now, scattering has been treated classically and the result of radiation interaction with "free" electrons.

This is not a good approximation since we know:

$$f(\vec{Q},\omega) = f^0(\vec{Q}) + f'(\omega) + if''(\omega)$$

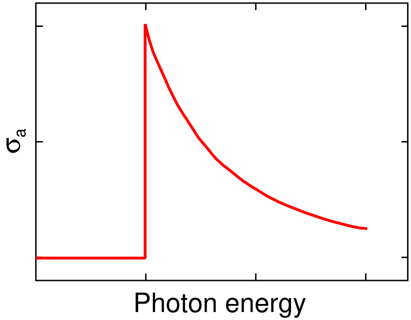

A better scattering model

Up to now, scattering has been treated classically and the result of radiation interaction with "free" electrons.

This is not a good approximation since we know:

$$f(\vec{Q}, \omega) = f^0(\vec{Q}) + f'(\omega) + if''(\omega)$$

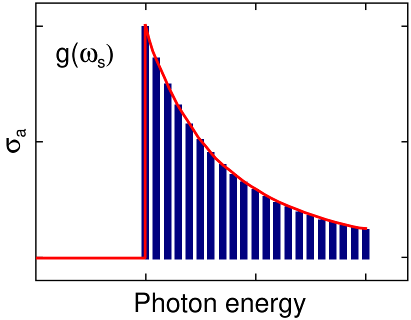

The absorption cross section can be modeled as a sum of forced, dissipative oscillators with distribution $g(\omega_s)$.

A better scattering model

Up to now, scattering has been treated classically and the result of radiation interaction with "free" electrons.

This is not a good approximation since we know:

$$f(\vec{Q},\omega) = f^0(\vec{Q}) + f'(\omega) + if''(\omega)$$

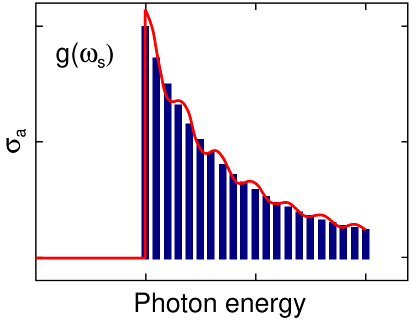

The absorption cross section can be modeled as a sum of forced, dissipative oscillators with distribution $g(\omega_s)$.

This will produce the resonant scattering term but not the XANES and EXAFS, which are purely quantum effects.

Forced charged oscillator

Consider an electron under the influence of an oscillating electric field $\vec{E}_{in} = \hat{x} E_0 e^{-i\omega t}$.

Forced charged oscillator

Consider an electron under the influence of an oscillating electric field $\vec{E}_{in} = \hat{x}E_0 e^{-i\omega t}$.

$$\ddot{x} + \Gamma\dot{x} + \omega_s^2 x = -\left(\frac{eE_0}{m}\right) e^{-i\omega t}$$

Forced charged oscillator

Consider an electron under the influence of an oscillating electric field $\vec{E}_{in} = \hat{x}E_0 e^{-i\omega t}$.

$$\ddot{x} + \Gamma\dot{x} + \omega_s^2 x = -\left(\frac{eE_0}{m}\right) e^{-i\omega t}$$

where Γ is the damping constant, ω_s is the resonant frequency of the oscillator, and $\Gamma \ll \omega_s$.

Forced charged oscillator

Consider an electron under the influence of an oscillating electric field $\vec{E}_{in} = \hat{x}E_0 e^{-i\omega t}$.

$$\ddot{x} + \Gamma\dot{x} + \omega_s^2 x = -\left(\frac{eE_0}{m}\right) e^{-i\omega t}$$

where Γ is the damping constant, ω_s is the resonant frequency of the oscillator, and $\Gamma \ll \omega_s$.

assuming a solution of the form

Forced charged oscillator

Consider an electron under the influence of an oscillating electric field $\vec{E}_{in} = \hat{x}E_0 e^{-i\omega t}$.

$$\ddot{x} + \Gamma\dot{x} + \omega_s^2 x = -\left(\frac{eE_0}{m}\right) e^{-i\omega t}$$

where Γ is the damping constant, ω_s is the resonant frequency of the oscillator, and $\Gamma \ll \omega_s$.

assuming a solution of the form

$$x = x_0 e^{-i\omega t}$$

Forced charged oscillator

Consider an electron under the influence of an oscillating electric field $\vec{E}_{in} = \hat{x} E_0 e^{-i\omega t}$.

where Γ is the damping constant, ω_s is the resonant frequency of the oscillator, and $\Gamma \ll \omega_s$.

assuming a solution of the form

$$\ddot{x} + \Gamma \dot{x} + \omega_s^2 x = -\left(\frac{eE_0}{m}\right) e^{-i\omega t}$$

$$x = x_0 e^{-i\omega t}$$

$$\dot{x} = -i\omega x_0 e^{-i\omega t}$$

Forced charged oscillator

Consider an electron under the influence of an oscillating electric field $\vec{E}_{in} = \hat{x} E_0 e^{-i\omega t}$.

$$\ddot{x} + \Gamma \dot{x} + \omega_s^2 x = -\left(\frac{eE_0}{m}\right) e^{-i\omega t}$$

where Γ is the damping constant, ω_s is the resonant frequency of the oscillator, and $\Gamma \ll \omega_s$.

assuming a solution of the form

$$x = x_0 e^{-i\omega t}$$

$$\dot{x} = -i\omega x_0 e^{-i\omega t}$$

$$\ddot{x} = -\omega^2 x_0 e^{-i\omega t}$$

Forced charged oscillator

Consider an electron under the influence of an oscillating electric field $\vec{E}_{in} = \hat{x}E_0 e^{-i\omega t}$.

$$\ddot{x} + \Gamma\dot{x} + \omega_s^2 x = -\left(\frac{eE_0}{m}\right) e^{-i\omega t}$$

where Γ is the damping constant, ω_s is the resonant frequency of the oscillator, and $\Gamma \ll \omega_s$.

assuming a solution of the form

$$x = x_0 e^{-i\omega t}$$
$$\dot{x} = -i\omega x_0 e^{-i\omega t}$$
$$\ddot{x} = -\omega^2 x_0 e^{-i\omega t}$$

$$(-\omega^2 - i\omega\Gamma + \omega_s^2)x_0 e^{-i\omega t} = -\left(\frac{eE_0}{m}\right) e^{-i\omega t}$$

Forced charged oscillator

Consider an electron under the influence of an oscillating electric field $\vec{E}_{in} = \hat{x}E_0 e^{-i\omega t}$.

$$\ddot{x} + \Gamma\dot{x} + \omega_s^2 x = -\left(\frac{eE_0}{m}\right)e^{-i\omega t}$$

where Γ is the damping constant, ω_s is the resonant frequency of the oscillator, and $\Gamma \ll \omega_s$.

assuming a solution of the form

$$x = x_0 e^{-i\omega t}$$

$$\dot{x} = -i\omega x_0 e^{-i\omega t}$$

$$\ddot{x} = -\omega^2 x_0 e^{-i\omega t}$$

$$(-\omega^2 - i\omega\Gamma + \omega_s^2)x_0 e^{-i\omega t} = -\left(\frac{eE_0}{m}\right)e^{-i\omega t}$$

$$x_0 = -\left(\frac{eE_0}{m}\right)\frac{1}{(\omega_s^2 - \omega^2 - i\omega\Gamma)}$$

Forced charged oscillator

Consider an electron under the influence of an oscillating electric field $\vec{E}_{in} = \hat{x}E_0 e^{-i\omega t}$.

$$\ddot{x} + \Gamma\dot{x} + \omega_s^2 x = -\left(\frac{eE_0}{m}\right) e^{-i\omega t}$$

where Γ is the damping constant, ω_s is the resonant frequency of the oscillator, and $\Gamma \ll \omega_s$.

assuming a solution of the form

$$x = x_0 e^{-i\omega t}$$

$$\dot{x} = -i\omega x_0 e^{-i\omega t}$$

$$\ddot{x} = -\omega^2 x_0 e^{-i\omega t}$$

$$(-\omega^2 - i\omega\Gamma + \omega_s^2)x_0 e^{-i\omega t} = -\left(\frac{eE_0}{m}\right) e^{-i\omega t}$$

$$x_0 = -\left(\frac{eE_0}{m}\right)\frac{1}{(\omega_s^2 - \omega^2 - i\omega\Gamma)}$$

The amplitude of the response has a resonance and dissipation

Radiated field

The radiated (scattered) electric field at a distance R from the electron is directly proportional to the electron's acceleration with a retarded time $t' = t - R/c$ (allowing for the travel time to the detector).

Radiated field

The radiated (scattered) electric field at a distance R from the electron is directly proportional to the electron's acceleration with a retarded time $t' = t - R/c$ (allowing for the travel time to the detector).

$$E_{rad}(R,t) = \left(\frac{e}{4\pi\epsilon_0 R c^2}\right)\ddot{x}(t - R/c)$$

Radiated field

The radiated (scattered) electric field at a distance R from the electron is directly proportional to the electron's acceleration with a retarded time $t' = t - R/c$ (allowing for the travel time to the detector).

$$E_{rad}(R,t) = \left(\frac{e}{4\pi\epsilon_0 Rc^2}\right)\ddot{x}(t - R/c) = \left(\frac{e}{4\pi\epsilon_0 Rc^2}\right)(-\omega^2)x_0 e^{-i\omega t}e^{i\omega R/c}$$

Radiated field

The radiated (scattered) electric field at a distance R from the electron is directly proportional to the electron's acceleration with a retarded time $t' = t - R/c$ (allowing for the travel time to the detector).

$$E_{rad}(R,t) = \left(\frac{e}{4\pi\epsilon_0 Rc^2}\right)\ddot{x}(t-R/c) = \left(\frac{e}{4\pi\epsilon_0 Rc^2}\right)(-\omega^2)x_0 e^{-i\omega t}e^{i\omega R/c}$$
$$= \frac{\omega^2}{(\omega_s^2 - \omega^2 - i\omega\Gamma)}\left(\frac{e^2}{4\pi\epsilon_0 mc^2}\right)E_0 e^{-i\omega t}\left(\frac{e^{ikR}}{R}\right)$$

Radiated field

The radiated (scattered) electric field at a distance R from the electron is directly proportional to the electron's acceleration with a retarded time $t' = t - R/c$ (allowing for the travel time to the detector).

$$E_{rad}(R,t) = \left(\frac{e}{4\pi\epsilon_0 Rc^2}\right)\ddot{x}(t-R/c) = \left(\frac{e}{4\pi\epsilon_0 Rc^2}\right)(-\omega^2)x_0 e^{-i\omega t}e^{i\omega R/c}$$

$$= \frac{\omega^2}{(\omega_s^2 - \omega^2 - i\omega\Gamma)}\left(\frac{e^2}{4\pi\epsilon_0 mc^2}\right)E_0 e^{-i\omega t}\left(\frac{e^{ikR}}{R}\right)$$

$$\frac{E_{rad}(R,t)}{E_{in}} = -r_0\frac{\omega^2}{(\omega^2 - \omega_s^2 + i\omega\Gamma)}\left(\frac{e^{ikR}}{R}\right)$$

Radiated field

The radiated (scattered) electric field at a distance R from the electron is directly proportional to the electron's acceleration with a retarded time $t' = t - R/c$ (allowing for the travel time to the detector).

$$E_{rad}(R,t) = \left(\frac{e}{4\pi\epsilon_0 Rc^2}\right)\ddot{x}(t - R/c) = \left(\frac{e}{4\pi\epsilon_0 Rc^2}\right)(-\omega^2)x_0 e^{-i\omega t}e^{i\omega R/c}$$

$$= \frac{\omega^2}{(\omega_s^2 - \omega^2 - i\omega\Gamma)}\left(\frac{e^2}{4\pi\epsilon_0 mc^2}\right)E_0 e^{-i\omega t}\left(\frac{e^{ikR}}{R}\right)$$

$$\frac{E_{rad}(R,t)}{E_{in}} = -r_0\frac{\omega^2}{(\omega^2 - \omega_s^2 + i\omega\Gamma)}\left(\frac{e^{ikR}}{R}\right) = -r_0 f_s\left(\frac{e^{ikR}}{R}\right)$$

Radiated field

The radiated (scattered) electric field at a distance R from the electron is directly proportional to the electron's acceleration with a retarded time $t' = t - R/c$ (allowing for the travel time to the detector).

$$E_{rad}(R,t) = \left(\frac{e}{4\pi\epsilon_0 Rc^2}\right)\ddot{x}(t - R/c) = \left(\frac{e}{4\pi\epsilon_0 Rc^2}\right)(-\omega^2)x_0 e^{-i\omega t} e^{i\omega R/c}$$
$$= \frac{\omega^2}{(\omega_s^2 - \omega^2 - i\omega\Gamma)}\left(\frac{e^2}{4\pi\epsilon_0 mc^2}\right)E_0 e^{-i\omega t}\left(\frac{e^{ikR}}{R}\right)$$

$$\frac{E_{rad}(R,t)}{E_{in}} = -r_0\frac{\omega^2}{(\omega^2 - \omega_s^2 + i\omega\Gamma)}\left(\frac{e^{ikR}}{R}\right) = -r_0 f_s\left(\frac{e^{ikR}}{R}\right)$$

which is an outgoing spherical wave with scattering amplitude

Radiated field

The radiated (scattered) electric field at a distance R from the electron is directly proportional to the electron's acceleration with a retarded time $t' = t - R/c$ (allowing for the travel time to the detector).

$$E_{rad}(R,t) = \left(\frac{e}{4\pi\epsilon_0 Rc^2}\right)\ddot{x}(t - R/c) = \left(\frac{e}{4\pi\epsilon_0 Rc^2}\right)(-\omega^2)x_0 e^{-i\omega t}e^{i\omega R/c}$$

$$= \frac{\omega^2}{(\omega_s^2 - \omega^2 - i\omega\Gamma)}\left(\frac{e^2}{4\pi\epsilon_0 mc^2}\right)E_0 e^{-i\omega t}\left(\frac{e^{ikR}}{R}\right)$$

$$\frac{E_{rad}(R,t)}{E_{in}} = -r_0\frac{\omega^2}{(\omega^2 - \omega_s^2 + i\omega\Gamma)}\left(\frac{e^{ikR}}{R}\right) = -r_0 f_s\left(\frac{e^{ikR}}{R}\right)$$

which is an outgoing spherical wave with scattering amplitude

$$f_s = \frac{\omega^2}{(\omega^2 - \omega_s^2 + i\omega\Gamma)}$$

Dispersion corrections

The scattering factor can be rewritten

$$f_s = \frac{\omega^2}{(\omega^2 - \omega_s^2 + i\omega\Gamma)}$$

Dispersion corrections

The scattering factor can be rewritten

$$f_s = \frac{\omega^2 + (-\omega_s^2 + i\omega\Gamma) - (-\omega_s^2 + i\omega\Gamma)}{(\omega^2 - \omega_s^2 + i\omega\Gamma)}$$

Dispersion corrections

The scattering factor can be rewritten

$$f_s = \frac{\omega^2 + (-\omega_s^2 + i\omega\Gamma) - (-\omega_s^2 + i\omega\Gamma)}{(\omega^2 - \omega_s^2 + i\omega\Gamma)}$$

$$= 1 + \frac{\omega_s^2 - i\omega\Gamma}{(\omega^2 - \omega_s^2 + i\omega\Gamma)}$$

Dispersion corrections

The scattering factor can be rewritten

$$f_s = \frac{\omega^2 + (-\omega_s^2 + i\omega\Gamma) - (-\omega_s^2 + i\omega\Gamma)}{(\omega^2 - \omega_s^2 + i\omega\Gamma)}$$

and since $\Gamma \ll \omega_s$

$$= 1 + \frac{\omega_s^2 - i\omega\Gamma}{(\omega^2 - \omega_s^2 + i\omega\Gamma)}$$

Dispersion corrections

The scattering factor can be rewritten

$$f_s = \frac{\omega^2 + (-\omega_s^2 + i\omega\Gamma) - (-\omega_s^2 + i\omega\Gamma)}{(\omega^2 - \omega_s^2 + i\omega\Gamma)}$$

and since $\Gamma \ll \omega_s$

$$= 1 + \frac{\omega_s^2 - i\omega\Gamma}{(\omega^2 - \omega_s^2 + i\omega\Gamma)} \approx 1 + \frac{\omega_s^2}{(\omega^2 - \omega_s^2 + i\omega\Gamma)}$$

Dispersion corrections

The scattering factor can be rewritten

$$f_s = \frac{\omega^2 + (-\omega_s^2 + i\omega\Gamma) - (-\omega_s^2 + i\omega\Gamma)}{(\omega^2 - \omega_s^2 + i\omega\Gamma)}$$

and since $\Gamma \ll \omega_s$

$$= 1 + \frac{\omega_s^2 - i\omega\Gamma}{(\omega^2 - \omega_s^2 + i\omega\Gamma)} \approx 1 + \frac{\omega_s^2}{(\omega^2 - \omega_s^2 + i\omega\Gamma)}$$

the second term being the dispersion correction

Dispersion corrections

The scattering factor can be rewritten

$$f_s = \frac{\omega^2 + (-\omega_s^2 + i\omega\Gamma) - (-\omega_s^2 + i\omega\Gamma)}{(\omega^2 - \omega_s^2 + i\omega\Gamma)}$$

and since $\Gamma \ll \omega_s$

$$= 1 + \frac{\omega_s^2 - i\omega\Gamma}{(\omega^2 - \omega_s^2 + i\omega\Gamma)} \approx 1 + \frac{\omega_s^2}{(\omega^2 - \omega_s^2 + i\omega\Gamma)}$$

the second term being the dispersion correction

$$\chi(\omega) = f_s' + if_s''$$

Dispersion corrections

The scattering factor can be rewritten

$$f_s = \frac{\omega^2 + (-\omega_s^2 + i\omega\Gamma) - (-\omega_s^2 + i\omega\Gamma)}{(\omega^2 - \omega_s^2 + i\omega\Gamma)}$$

and since $\Gamma \ll \omega_s$

$$= 1 + \frac{\omega_s^2 - i\omega\Gamma}{(\omega^2 - \omega_s^2 + i\omega\Gamma)} \approx 1 + \frac{\omega_s^2}{(\omega^2 - \omega_s^2 + i\omega\Gamma)}$$

the second term being the dispersion correction

$$\chi(\omega) = f_s' + i f_s'' = \frac{\omega_s^2}{(\omega^2 - \omega_s^2 + i\omega\Gamma)}$$

Dispersion corrections

The scattering factor can be rewritten

$$f_s = \frac{\omega^2 + (-\omega_s^2 + i\omega\Gamma) - (-\omega_s^2 + i\omega\Gamma)}{(\omega^2 - \omega_s^2 + i\omega\Gamma)}$$

and since $\Gamma \ll \omega_s$

$$= 1 + \frac{\omega_s^2 - i\omega\Gamma}{(\omega^2 - \omega_s^2 + i\omega\Gamma)} \approx 1 + \frac{\omega_s^2}{(\omega^2 - \omega_s^2 + i\omega\Gamma)}$$

the second term being the dispersion correction whose real and imaginary components can be extracted

$$\chi(\omega) = f_s' + i f_s'' = \frac{\omega_s^2}{(\omega^2 - \omega_s^2 + i\omega\Gamma)}$$

Dispersion corrections

The scattering factor can be rewritten

$$f_s = \frac{\omega^2 + (-\omega_s^2 + i\omega\Gamma) - (-\omega_s^2 + i\omega\Gamma)}{(\omega^2 - \omega_s^2 + i\omega\Gamma)}$$

and since $\Gamma \ll \omega_s$

$$= 1 + \frac{\omega_s^2 - i\omega\Gamma}{(\omega^2 - \omega_s^2 + i\omega\Gamma)} \approx 1 + \frac{\omega_s^2}{(\omega^2 - \omega_s^2 + i\omega\Gamma)}$$

the second term being the dispersion correction whose real and imaginary components can be extracted

$$\chi(\omega) = f_s' + if_s'' = \frac{\omega_s^2}{(\omega^2 - \omega_s^2 + i\omega\Gamma)}$$

$$\chi(\omega) = \frac{\omega_s^2}{(\omega^2 - \omega_s^2 + i\omega\Gamma)} \cdot \frac{(\omega^2 - \omega_s^2 - i\omega\Gamma)}{(\omega^2 - \omega_s^2 - i\omega\Gamma)}$$

Dispersion corrections

The scattering factor can be rewritten

$$f_s = \frac{\omega^2 + (-\omega_s^2 + i\omega\Gamma) - (-\omega_s^2 + i\omega\Gamma)}{(\omega^2 - \omega_s^2 + i\omega\Gamma)}$$

and since $\Gamma \ll \omega_s$

$$= 1 + \frac{\omega_s^2 - i\omega\Gamma}{(\omega^2 - \omega_s^2 + i\omega\Gamma)} \approx 1 + \frac{\omega_s^2}{(\omega^2 - \omega_s^2 + i\omega\Gamma)}$$

the second term being the dispersion correction whose real and imaginary components can be extracted

$$\chi(\omega) = f_s' + if_s'' = \frac{\omega_s^2}{(\omega^2 - \omega_s^2 + i\omega\Gamma)}$$

$$\chi(\omega) = \frac{\omega_s^2}{(\omega^2 - \omega_s^2 + i\omega\Gamma)} \cdot \frac{(\omega^2 - \omega_s^2 - i\omega\Gamma)}{(\omega^2 - \omega_s^2 - i\omega\Gamma)} = \frac{\omega_s^2(\omega^2 - \omega_s^2 - i\omega\Gamma)}{(\omega^2 - \omega_s^2)^2 + (\omega\Gamma)^2}$$

Dispersion corrections

The scattering factor can be rewritten

$$f_s = \frac{\omega^2 + (-\omega_s^2 + i\omega\Gamma) - (-\omega_s^2 + i\omega\Gamma)}{(\omega^2 - \omega_s^2 + i\omega\Gamma)}$$

and since $\Gamma \ll \omega_s$

$$= 1 + \frac{\omega_s^2 - i\omega\Gamma}{(\omega^2 - \omega_s^2 + i\omega\Gamma)} \approx 1 + \frac{\omega_s^2}{(\omega^2 - \omega_s^2 + i\omega\Gamma)}$$

the second term being the dispersion correction whose real and imaginary components can be extracted

$$\chi(\omega) = f_s' + if_s'' = \frac{\omega_s^2}{(\omega^2 - \omega_s^2 + i\omega\Gamma)}$$

$$\chi(\omega) = \frac{\omega_s^2}{(\omega^2 - \omega_s^2 + i\omega\Gamma)} \cdot \frac{(\omega^2 - \omega_s^2 - i\omega\Gamma)}{(\omega^2 - \omega_s^2 - i\omega\Gamma)} = \frac{\omega_s^2(\omega^2 - \omega_s^2 - i\omega\Gamma)}{(\omega^2 - \omega_s^2)^2 + (\omega\Gamma)^2}$$

$$f_s' = \frac{\omega_s^2(\omega^2 - \omega_s^2)}{(\omega^2 - \omega_s^2)^2 + (\omega\Gamma)^2}$$

Dispersion corrections

The scattering factor can be rewritten

$$f_s = \frac{\omega^2 + (-\omega_s^2 + i\omega\Gamma) - (-\omega_s^2 + i\omega\Gamma)}{(\omega^2 - \omega_s^2 + i\omega\Gamma)}$$

and since $\Gamma \ll \omega_s$

$$= 1 + \frac{\omega_s^2 - i\omega\Gamma}{(\omega^2 - \omega_s^2 + i\omega\Gamma)} \approx 1 + \frac{\omega_s^2}{(\omega^2 - \omega_s^2 + i\omega\Gamma)}$$

the second term being the dispersion correction whose real and imaginary components can be extracted

$$\chi(\omega) = f_s' + if_s'' = \frac{\omega_s^2}{(\omega^2 - \omega_s^2 + i\omega\Gamma)}$$

$$\chi(\omega) = \frac{\omega_s^2}{(\omega^2 - \omega_s^2 + i\omega\Gamma)} \cdot \frac{(\omega^2 - \omega_s^2 - i\omega\Gamma)}{(\omega^2 - \omega_s^2 - i\omega\Gamma)} = \frac{\omega_s^2(\omega^2 - \omega_s^2 - i\omega\Gamma)}{(\omega^2 - \omega_s^2)^2 + (\omega\Gamma)^2}$$

$$f_s' = \frac{\omega_s^2(\omega^2 - \omega_s^2)}{(\omega^2 - \omega_s^2)^2 + (\omega\Gamma)^2} \qquad f_s'' = -\frac{\omega_s^2\omega\Gamma}{(\omega^2 - \omega_s^2)^2 + (\omega\Gamma)^2}$$

Single oscillator dispersion terms

These dispersion terms give resonant corrections to the scattering factor

Single oscillator dispersion terms

These dispersion terms give resonant corrections to the scattering factor

$$f_s' = \frac{\omega_s^2(\omega^2 + \omega_s^2)}{(\omega^2 - \omega_s^2)^2 + (\omega\Gamma)^2}$$

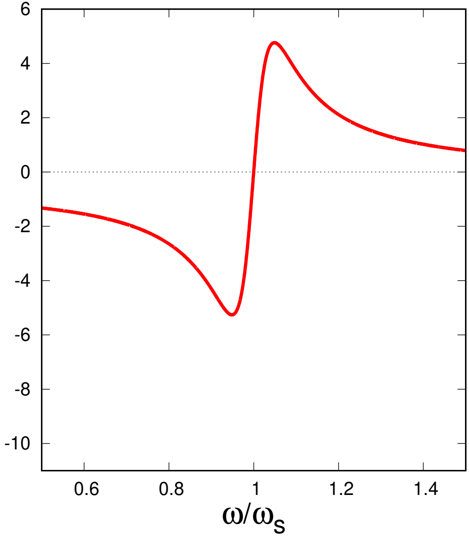

Single oscillator dispersion terms

These dispersion terms give resonant corrections to the scattering factor

$$f'_s = \frac{\omega_s^2(\omega^2+\omega_s^2)}{(\omega^2-\omega_s^2)^2+(\omega\Gamma)^2}$$

$$f''_s = -\frac{\omega_s^2\omega\Gamma}{(\omega^2-\omega_s^2)^2+(\omega\Gamma)^2}$$